4940 *Inorg. Chem.* **1993,** *32,* 4940–4950

# Ruthenium(II) Complexes Containing Bis(2-(diphenylphosphino)ethyl)phenylphosphine and Bis(3-(diphenylphosphino)propyl)phenylphosphine

**Alberto Albinati,[†] Qiongzhong Jiang,[‡] Heinz Rüegger,[‡] and Luigi M. Venanzi*,[‡]**

Laboratorium für Anorganische Chemie der Eidgenössischen Technischen Hochschule, ETH Zentrum, Universitätstrasse 6, CH-8092 Zürich, Switzerland, and Istituto di Chimica Farmaceutica dell' Università di Milano, Viale Abruzzi 42, I-20131 Milano, Italy

*Received April 6, 1993*[⊗]

A compound of composition “RuCl$_2$(ETP)” (ETP = bis(2-(diphenylphosphino)ethyl)phenylphosphine) has been shown to contain the binuclear cation [Ru$_2$($\mu$-Cl)$_3$(ETP)$_2$]$^+$ and Cl$^-$. In CDCl$_3$, the cation is present as a mixture of the staggered and eclipsed isomeric forms. The X-ray crystal structure of [Ru$_2$($\mu$-Cl)$_3$(ETP)$_2$](CF$_3$SO$_3$) shows that only the eclipsed form is present in the single crystals grown from CH$_2$Cl$_2$/CHCl$_3$/PhMe. The *tri*solvento complex [Ru(MeCN)$_3$(ETP)](CF$_3$SO$_3$)$_2$ was isolated and its X-ray crystal structure was determined. The ETP ligand in this complex retains facial coordination. It is found that a CDCl$_3$ solution of this complex also contains the monocationic *di*solvento complex, i.e., [Ru(CF$_3$SO$_3$)(MeCN)$_2$(ETP)](CF$_3$SO$_3$). The compound “RuCl$_2$(TTP)” (TTP = bis(3-(diphenylphosphino)propyl)phenylphosphine) was structurally characterized by X-ray diffraction and found to be a mononuclear five-coordinate complex with a geometry which is intermediate between square pyramidal and trigonal bipyramidal. It was also found that, in MeCN solution, *fac*-[RuCl$_2$(TTP)] gives octahedral *fac*-[RuCl(MeCN)$_2$(TTP)]$^+$ in which the TTP ligand maintains facial coordination. The latter structural feature is also present in *fac*-[Ru(MeCN)$_3$(TTP)]$^{2+}$.

## Introduction

Cationic solvento complexes of the platinum metals containing bi- or terdentate phosphine ligands are beginning to find increasing use as acetalization catalysts.[1] The main advantages of these catalysts are (1) their activity is often superior to those of protonic acids,[1a,b] (2) they can be used for the acetalization of acid-sensitive organic carbonyl compounds,[1a,b] and (3) they show diastereoselectivities which are different from those of protonic acids.[1a,b] Furthermore, catalysts of this type can be readily modified by changing the size and shape of their “active sites”, which can also be made chiral.

The most extensively studied acetalization catalysts containing platinum metals are those of rhodium(III) coordinated to the tripodal ligand 1,1,1-tris((diphenylphosphino)methyl)ethane, TRIPHOS, the most active compound being [Rh(MeCN)$_3$(TRIPHOS)](CF$_3$SO$_3$)$_3$ (**1**).[1a,b]

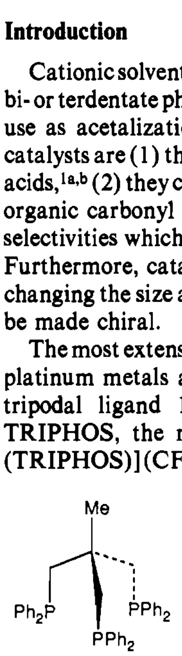
TRIPHOS

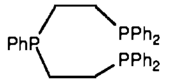
ETP

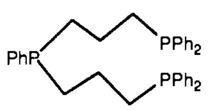
TTP

However, these investigations indicate that (a) the corresponding ruthenium(II) cation, i.e., [Ru(MeCN)$_3$(TRIPHOS)](CF$_3$SO$_3$)$_2$ (**2**),[2] should also be catalytically active and (b) it might even be possible to use complexes of chainlike terdentate ligands such as bis(2-(diphenylphosphino)ethyl)phenylphosphine, ETP, or bis(3-(diphenylphosphino)propyl)phenylphosphine, TTP, i.e., *fac*-[Ru(MeCN)$_3$(LLL)]$^{2+}$ (LLL = ETP (**3**), TTP (**4**)), as catalyst precursors instead of those of TRIPHOS.

The use of ruthenium instead of rhodium has the advantage that the former is considerably less expensive than the latter. Furthermore, structural variations can be more conveniently made in chainlike ligands than in tripodal ligands and, thus, it should be easier to significantly influence the diastereoselectivities of reactions of interest. Finally, ligands such as ETP are commercially available.

While the catalytic experiments using cationic complexes of the type [Ru(MeCN)$_3$(LLL)](CF$_3$SO$_3$)$_2$ (LLL = TRIPHOS, ETP, TTP) will be described elsewhere, we report here (1) a reinvestigation of the complexes “RuCl$_2$(ETP)” (**5**) and “RuCl$_2$(TTP)” (**6**), (2) the preparation and characterization of the cationic solvento complexes [Ru(MeCN)$_3$(ETP)](CF$_3$SO$_3$)$_2$ (**3**), [Ru(CF$_3$SO$_3$)(MeCN)$_2$(ETP)](CF$_3$SO$_3$) (**7**), and *fac*-[Ru(MeCN)$_3$(TTP)](CF$_3$SO$_3$)$_2$ (**4**), required as catalyst precursors for the acetalization reaction, (3) the X-ray crystal structures of *ec*-[Ru$_2$($\mu$-Cl)$_3$(ETP)$_2$](CF$_3$SO$_3$) (*ec* = eclipsed) (**5a**), [Ru(MeCN)$_3$(ETP)](CF$_3$SO$_3$)$_2$ (**3**), and *fac*-[RuCl$_2$(TTP)] (**6**).

**ETP Complexes.** The coordination chemistry of ruthenium with ETP has been extensively investigated,[3-8] and a complex of the composition “RuCl$_2$(ETP)” (**5**) was obtained by a variety of

---

[†] Università di Milano.

[‡] ETH Zürich.

[⊗] Abstract published in *Advance ACS Abstracts,* October 1, 1993.

(1) (a) Ott, J.; Ramos Tombo, G. M.; Schmid, B.; Venanzi, L. M.; Wang, Q.; Ward, T. R. *Tetrahedron Lett.* **1989,** *30,* 6151. (b) Ott, J.; Schmid, B.; Venanzi, L. M.; Wang, G.; Ward, T. R.; Ramos Tombo, G. M. *New. J. Chem.* **1990,** *14,* 495. (c) Gorla, F.; Venanzi, L. M. *Helv. Chim. Acta* **1990,** *73,* 690. (d) Tani, K.; Fukui, Y.; Ise, T.; Tatsuno, M.; Saito,T. *Chem. Abstr.* **1988,** *108*: 21098b; JP 62,178,535 [87,178,535]. (e) Stille, J. K.; Su, H.; Brechot, P.; Parrinello, G.; Hegedus, L. S. *Organometallics* **1991,** *10,* 1183.

(2) (a) Sorato, C. Dissertation No. 8775, ETH Zürich, 1989. (b) Rhodes, L. F.; Sorato, C.; Venanzi, L. M.; Bachechi, F. *Inorg. Chem.* **1987,** *26,* 604.

(3) (a) King, R. B.; Kapoor, R. N.; Saran, M. S.; Kapoor, P. N. *Inorg. Chem.* **1971,** *10,* 841. (b) King, R. B.; Cloyd, J. C.; Reimann, R. H. *Inorg. Chem.* **1976,** *15,* 449.

(4) (a) Taqui Khan, M. M.; Mohiuddin, R. *J. Coord. Chem.* **1977,** *6,* 171. (b)Taqui Khan, M. M.; Taqui Khan, B.; Begum, S.; Ali, S. M. *J. Mol. Catal.* **1988,** *49,* 43.

(5) (a) Fontal, B. *Acta Cient. Venez.* **1982,** *33,* 202; *Chem. Abstr.* **1983,** *98,* 171876t. (b) Suarez, T.; Fontal, B.; Garcia, D. *Acta Cient. Venez.* **1983,** *34,* 198. (c) Suarez, T.; Fontal, B. *J. Mol. Catal.* **1985,** *32,* 191. (d) Suarez, T; Fontal, B. *J. Mol. Catal.* **1988,** *45,* 335.

(6) Davies, S. G.; Simpson, S. J.; Felkin, H.; Khan, T. F. *Organometallics* **1983,** *2,* 539 and references therein.

(7) Jia, Q.; Meek, D. W. *Inorg. Chim. Acta* **1990,** *178,* 195.

(8) Guimerans, R. G.; Hernandez, E. C.; Olmstead, M. M.; Balch, A. L. *Inorg. Chim. Acta* **1989,** *165,* 45.

0020-1669/93/1332-4940$04.00/0 © 1993 American Chemical Society

methods. Thus, (1) King *et al.*[3] prepared it from the direct reaction of $\mathrm{RuCl_3{\cdot}}n\mathrm{H_2O}$ and ETP in the presence of concentrated HCl (eq 1).

$$\mathrm{RuCl_3{\cdot}}n\mathrm{H_2O + ETP \xrightarrow{EtOH/conc\ HCl} “RuCl_2(ETP)”} \qquad (1)$$

They reported microanalytical data for their yellow compound, but they were unable to determine its molecular weight because of low solubility. The complex was formulated as a dimer with the structure

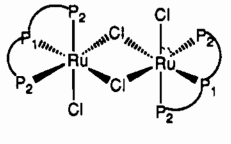

(2) Taqui Khan and co-workers[4] used $[\mathrm{RuCl_2(PPh_3)_3}]$ as the starting material for the preparation of **5** (eq 2). They described

$$\mathrm{[RuCl_2(PPh_3)_3] + ETP \xrightarrow[reflux]{benzene} “RuCl_2(ETP)”} \qquad (2)$$

their product as being "light green" in color. They also reported the presence of an IR absorption band at 332 $\mathrm{cm^{-1}}$ (m) and a $^1$H-NMR spectrum showing the presence of a multiplet centred at ca. 1 ppm assigned to the methylene protons of the organic ligand. Furthermore, they reported a molar conductance of 20 $\mathrm{ohm^{-1}\ cm^2\ equiv^{-1}}$ in dimethyl acetamide. On the basis of these data, they formulated their product as a monomer and proposed the structure.

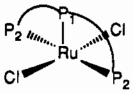

(3) Suarez and Fontal[5] obtained **5** starting from $[\mathrm{RuCl_2(DMSO)_4}]$(eq 3).

$$\mathrm{[RuCl_2(DMSO)_4] + ETP \xrightarrow[reflux]{toluene} “RuCl_2(ETP)”} \qquad (3)$$

Their yellow product was characterized by $^{31}$P-NMR ($\delta$(P) = 98.5 (t), and 68.5 ppm (d, $J$(P,P) = 22 Hz)). The microanalytical data given (both the calculated and found values) do not correspond to the above formulation, but are in closer agreement with the composition "$\mathrm{RuCl_2(ETP){\cdot}H_2O}$".

Finally, although several other ETP-containing ruthenium(II) complexes have been described,[3-9] the cationic solvento-complex $[\mathrm{Ru(MeCN)_3(ETP)}]^{2+}$ (**3**) does not appear to have been prepared.

**TTP Complexes.** Meek and co-workers[10d] reported the preparation of "$\mathrm{RuCl_2(TTP)}$", from $\mathrm{RuCl_3{\cdot}3H_2O}$ and TTP in methanol solution. They formulated their product as dimeric or polymeric on the basis of its low solubility and the presence of an infrared absorption band at 291 $\mathrm{cm^{-1}}$.

By abstracting chloride from "$\mathrm{RuCl_2(TTP)}$" with $\mathrm{Tl[AsF_6]}$ in acetonitrile, the same authors prepared a solvento complex, formulated as $[\mathrm{Ru(MeCN)_2(TTP)}][\mathrm{AsF_6}]_2$.[10d]

## Results and Discussion

**ETP Complexes.** Reactions 1–3 were carried out again. These gave yellow solids which were thoroughly investigated. Their microanalytical data did not agree with the composition "$\mathrm{RuCl_2(ETP)}$", even after the samples had been dried at ca. 130 °C under high vacuum for 12 h, but gave a better fit for the composition "$\mathrm{RuCl_2(ETP){\cdot}H_2O}$".

The IR spectra of the solids, obtained during the studies reported here, do not show bands assignable to terminal Ru–Cl stretching vibrations except for a very weak absorption at ca. 355 $\mathrm{cm^{-1}}$, but one observes an absorption band at 255 $\mathrm{cm^{-1}}$. This is consistent with the presence of Ru–Cl–Ru bridges, and thus, compound **5** is assigned the structure $[\mathrm{Ru_2(\mu\text{-}Cl)_3(ETP)_2}]\mathrm{Cl}$, with a cation similar to that found in $[\mathrm{Ru_2(\mu\text{-}Cl)_3(TRIPHOS)_2}][\mathrm{BPh_4}]$ (**11**)[2] and several complexes with monodentate phosphines, $[\mathrm{Ru_2(\mu\text{-}Cl)_3(PR_3)_6}]^+$.[11]

Confirmation of this structural assignment is provided by the FAB mass spectrum of **5** which gave a molecular ion at 1377, the mass of "$\mathrm{Ru_2(\mu\text{-}Cl)_3(ETP)_2}$" being 1377.6. Interestingly, the strongest fragment was found at 671, which corresponds exactly to the monomeric unit "RuCl(ETP)".

Finally, this binuclear cation has been found by X-ray diffraction in $[\mathrm{Ru_2(\mu\text{-}Cl)_3(ETP)_2}](\mathrm{CF_3SO_3})$ (see later).

A molecular weight determination of **5** (osmometric in $\mathrm{CH_2Cl_2}$) gives a value of 1506, approximately twice that calculated for "$\mathrm{RuCl_2(ETP)}$" (707). Compound **5** conducts in nitromethane and the value of the molar conductance, based on the dimeric formulation $[\mathrm{Ru_2(\mu\text{-}Cl)_3(ETP)_2}]\mathrm{Cl}$, is 69 $\mathrm{ohm^{-1}\ cm^2\ mol^{-1}}$, i.e., in the range for 1:1 electrolytes which, under the same conditions, give molar conductance values ranging from 60 to 115 $\mathrm{ohm^{-1}\ cm^2\ mol^{-1}}$.[12]

Confirmation of this structural assignment *in solution* is also provided by the following experiments: (1) one chloride ion is easily replaced by another anion, e.g., triflate, camphorsulfonate, and tetraphenylborate, giving solids of composition $[\mathrm{Ru_2(\mu\text{-}Cl)_3(ETP)_2}]\mathrm{Y}$ (Y = $\mathrm{CF_3SO_3}$ (**8**), camphorsulfonate (**9**), $\mathrm{BPh_4}$ (**10**)) with $^{31}$P-NMR spectra which are identical with those of the starting material **5** (see later and Table I); (2) the molar conductances of compounds **8**, **9** and **10**, in nitromethane, gave the values 61, 46, and 50 $\mathrm{ohm^{-1}\ cm^2\ mol^{-1}}$, respectively.

The $^{31}$P-NMR spectrum of **5**, in $\mathrm{CDCl_3}$, shows the presence of two species: one, **5a**, characterized by an $\mathrm{AX_2}$ splitting pattern with $\delta$(P) at 98.1 ppm (triplet) and 68.7 ppm (doublet) with $J$(P,P) = 23 Hz, and the other, **5b**, which gives a typical AMX splitting pattern, having (1) $\delta$(P) = 98.8 ppm (dd) with $J$(P,P) = 23.1 and 22.8 Hz, (2) $\delta$(P) = 70.8 ppm (dd) with $J$(P,P) = 29.3 and 22.8 Hz, and (3) $\delta$(P) = 66.6 ppm (dd) with $J$(P,P) = 29.3 and 23.1 Hz, respectively. Samples of **5** obtained by all of the above methods, in $\mathrm{CDCl_3}$, contained **5a** and **5b** in approximate ratios ranging from 2:1 to 2:1.6. Furthermore, a **5a**:**5b** isomer-ratio of 2:1.2 was obtained by adding 1.5 equiv of tetraphenylphosphonium chloride to a chloroform solution of 1 equiv of $[\mathrm{Ru(MeCN)_3(ETP)}](\mathrm{CF_3SO_3})_2$ (**3**) (see later).

The isomeric species **5a** and **5b** interchange fairly rapidly in solution. Although there does not appear to be any exchange at room temperature on the NMR time scale, this phenomenon is observed in $^{31}$P spin-inversion transfer experiments when a $\mathrm{CDCl_3}$ solution of this mixture is warmed up to 50 °C.

The above results are in apparent contrast with the report by Suarez and Fontal[5] of the observation of only one species in solution, i.e., that giving signals at $\delta$(P) = 98.5 (t) and 68.5 ppm (d) with $J$(P,P) = 22 Hz, which correspond to those observed for **5a**. However, their spectra were recorded at 1.4 T and, thus, it is possible that background noise may have masked the presence of the minor isomer.

The isomerism arises from the relative positions of the ETP-ligands in the binuclear cationic complexes, where the central P-atoms can either be eclipsed (*ec*-form) or staggered (*st*-form).

---

(9) Michos, D.; Luo, X.; Crabtree, R. H. *Inorg. Chem.* **1992**, *31*, 4245.

(10) (a) Meek, D. W.; Mazanec, T. J. *Acc. Chem. Res.* **1981**, *14*, 266. (b) Letts, J. B.; Mazanec, T. J.; Meek, D. W. *J. Am. Chem. Soc.* **1982**, *104*, 3898. (c) Letts, J. B.; Mazanec, T. J.; Meek, D. W. *J. Chem. Soc., Chem. Commun.* **1982**, 356. (d) Letts, J. B.; Mazanec, T. J.; Meek, D. W. *Organometallics* **1983**, *2*, 695. (e) Jia, Q.; Meek, D. W.; Gallucci, J. C. *Organometallics* **1990**, *9*, 2549. (f) Jia, Q.; Lee, I.; Meek, D. W.; Gallucci, J. C. *Inorg. Chim Acta* **1990**, *177*, 81. (g) Jia, Q.; Rheingold, A. L.; Haggerty, B. S.; Meek, D. W. *Inorg. Chem.* **1992**, *31*, 900.

(11) (a) Chatt, J.; Shaw, B. L.; Field, A. E. *J. Chem. Soc.* **1964**, 3466. (b) Cotton, F. A.; Torralba, R. C. *Inorg. Chem.* **1991**, *30*, 2196. (c) Statler, J. A.; Wilkinson, G.; Thornton-Pett, M.; Hursthouse, M. B. *J. Chem. Soc., Dalton Trans.* **1984**, 1731.

(12) Geary, W. J. *Coord. Chem. Rev.* **1971**, *7*, 81.

**Table I.** $^{31}$P-NMR Data for ETP and TTP Ruthenium Complexes

| | $^{31}$P{H}-NMR[a] | | | | | |
|---|---|---|---|---|---|---|
| complex | δ($P_c$) | δ($P_t^1$) | δ($P_t^2$) | J($P_cP_t^1$) | J($P_cP_t^2$) | J($P_t^1P_t^2$) |
| *ec*-[$Ru_2(\mu\text{-}Cl)_3(ETP)_2$]Cl (**5a**) | 98.1 (t) | 68.7 (d) | | 23.0 | | |
| *st*-[$Ru_2(\mu\text{-}Cl)_3(ETP)_2$]Cl (**5b**) | 98.8 (dd) | 70.8 (dd) | 66.6 (dd) | 22.8 | 23.1 | 29.3 |
| [$Ru_2(\mu\text{-}Cl)_3(ETP)_2$]Cl[b] (**5**) | 100 | 63 | 61 | | | |
| | 97 | 74 | 58 | | | |
| | 99 | 65 | 61 | | | |
| | 96 | 72 | 57 | | | |
| *ec*-[$Ru_2(\mu\text{-}Cl)_3(ETP)_2$]($CF_3SO_3$)[c] (**8a**) | 97.9 (t) | 68.2 (d) | | 22.8 | | |
| *st*-[$Ru_2(\mu\text{-}Cl)_3(ETP)_2$]($CF_3SO_3$)[c] (**8b**) | 98.4 (dd) | 70.0 (dd) | 66.3 (dd) | 23.0 | 23.2 | 29.0 |
| [$Ru_2(\mu\text{-}Cl)_3(ETP)_2$]($CF_3SO_3$)[b] (**8**) | 100 | 74 | 61 | | | |
| | 95 | 70 | 60 | | | |
| *ec*-[$Ru_2(\mu\text{-}Cl)_3(ETP)_2$](camphorsulfonate) (**9a**) | 98.2 (t) | 68.7 (d) | | 22.7 | | |
| *st*-[$Ru_2(\mu\text{-}Cl)_3(ETP)_2$](camphorsulfonate) (**9b**) | 98.9 (dd) | 70.9 (dd) | 66.6 (dd) | 22.3 | 23.2 | 28.9 |
| *ec*-[$Ru_2(\mu\text{-}Cl)_3(ETP)_2$][$BPh_4$][c] (**10a**) | 97.7 (t) | 68.4 (d) | | 22.7 | | |
| *st*-[$Ru_2(\mu\text{-}Cl)_3(ETP)_2$][$BPh_4$][c] (**10b**) | 98.2 (dd) | 70.0 (dd) | 66.4 (dd) | ca 23 | 23.1 | 28.9 |
| [$RuCl_2$(py)(ETP)] (**16**) | 96.4 (dd) | 60.1 (dd) | 59.6 (dd) | 18.1 | 17.4 | 30.1 |
| [Ru(MeCN)$_3$(ETP)]($CF_3SO_3$)$_2$[d,e] (**3**) | 97.8 (t) | 60.9 (d) | | 18.1 | | |
| [Ru(MeCN)$_3$(ETP)]($CF_3SO_3$)$_2$[b] (**3**) | 96 | 63 | 59 | | | |
| [Ru($CF_3SO_3$)(MeCN)$_2$(ETP)]($CF_3SO_3$) (**7**) | 104.4 (t) | 58.0 (d) | | 20.0 | | |
| *fac*-[$RuCl_2$(TTP)] (**6**) | | | (insoluble in non-coordinating solvents) | | | |
| *fac*-[RuCl(MeCN)$_2$(TTP)]Cl[f] (**17**) | 18.2 (dd) | 28.2 (dd) | 25.8 (dd) | 39.6 | 46.8 | 27.7 |
| *fac*-[Ru(MeCN)$_3$(TTP)]($CF_3SO_3$)$_2$ (**4**) | 17.6 (t) | 23.6 (d) | | 41.9 | | |
| [RuCl(MeCN)$_2$(ETP)]($CF_3SO_3$)[d] (**12**) | 100.4 (t) | 58.2 (d) | | 18.1 | | |
| [RuCl(MeCN)$_2$(ETP)]Cl[d] (**13**) | 100.6 (t) | 58.3 (d) | | 18.0 | | |
| [$RuCl_2$(MeCN)(ETP)][d,h] (**14**) | 102.1 (dd) | 62.1 (dd) | 59.9 (dd) | 21.0 | 16.0 | 32.8 |
| [RuCl(MeCN)$_2$(ETP)]Cl[d,g] (**15**) | 99.1 (dd) | 64.7 (dd) | 63.9 (dd) | 17.3 | 19.4 | 28.6 |

[a] Chemical shifts in δ (ppm) with respect to 85% $H_3PO_4$; positive values denote downfield shifts relative to the reference; coupling constants in Hz (s = singlet, d = doublet, dd = doublet of doublets, t = triplet); unless otherwise noted the solvent was $CDCl_3$. [b] In solid state. [c] In $CDCl_3/CH_2Cl_2$. [d] In $CD_3CN$. [e] When recorded in $CDCl_3$, the spectrum of this compound showed resonances at δ(P) = 97.6 (t) and 60.2 ppm (d) for **3** as well as those for **7** at 104.3 (t) and 58.1 (d) ppm. [f] In $CDCl_3$/MeCN. [g] At 0 °C. [h] At −20 °C.

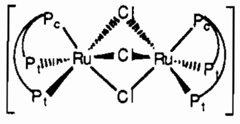

(**5a**) (*ec*-form)

and

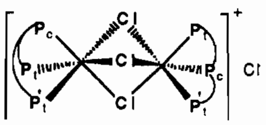

(**5b**) (*st*-form)

The $^{31}$P-NMR data, in $CDCl_3$ solution, for these isomers allow the unambiguous assignments to the corresponding structures shown above. Thus, the structure **5a**, is assigned to the isomer characterized by δ(P) values at 98.1 (t) and 68.7 ppm (d, J(P,P) = 23.0 Hz), as the presence of a plane of symmetry bisecting the $P_c$ and Ru atoms renders the $P_t$ donors chemically equivalent and therefore, gives rise to a single signal, although they are magnetically nonequivalent (AA′A″A‴XX′ spin system). On the other hand, due to the absence of any symmetry element in isomer **5b**, the terminal $P_t$ atoms of ETP are not equivalent and should give rise to two $^{31}$P-NMR signals with their relative coupling constants, as found for this isomer with δ(P) values at 98.8 (dd, J(P,P) = 23.1 and 22.8 Hz), 70.8 (dd, J(P,P) = 29.3 and 22.8 Hz), and 66.6 ppm (dd, J(P,P) = 29.3 and 23.1 Hz) (see Table I). The respective J(P,P) coupling constants prove the facial coordination of ETP, i.e., these data are inconsistent with the mononuclear formulation proposed by Taqui Kahn and co-workers.[4]

It should be noted that the *ec*-isomer (**5a**) is a *meso*-form, whereas the *st*-isomer (**5b**) is chiral and should be present as an enantiomeric pair. Investigations of the complex cations [$Ru_2(\mu\text{-}Cl)_3(ETP^*)_2$]$^+$ (ETP* = (1*R*)-(−)-menthyl-P($CH_2CH_2PPh_2)_2$), which should show the presence of three distinguishable diastereoisomers, are in progress.[13]

**X-ray Crystal Structure of *ec*-[$Ru_2(\mu\text{-}Cl)_3(ETP)_2$]($CF_3SO_3$)·$CH_2Cl_2$ (8a·$CH_2Cl_2$).** The crystals contain a binuclear cation and a triflate anion without significant contacts between them. An ORTEP drawing of the complex cation is shown in Figure 1, and a selection of bond lengths and angles is given in Table II.

The metal coordination is cofacial bioctahedral, with three bridging chlorine atoms, the other three coordination sites on each ruthenium atom being occupied by the terdentate phosphine. As mentioned earlier, this type of coordination has been frequently observed in ruthenium chemistry. The bonding parameters in **8a** are comparable with those of the related compounds with monodentate phosphine ligands and, in particular, with [$Ru_2(\mu\text{-}Cl)_3(TRIPHOS)_2$][$BPh_4$] (**11**)[2b] (see Table II). However, there are several significant differences. Thus, the Ru–P distances fall into three groups: (1) those to the central $P_c$ atoms which are the shortest (2.251(2) (average) Å), (2) those to two terminal $P_t$ atoms which are 2.266(2) (average) Å, and (3) those to the other two terminal $P_t$ atoms which are 2.287(5) (average) Å. It is noteworthy that all of them are shorter than the Ru–P distances in **11** (2.305(7) (average) Å).

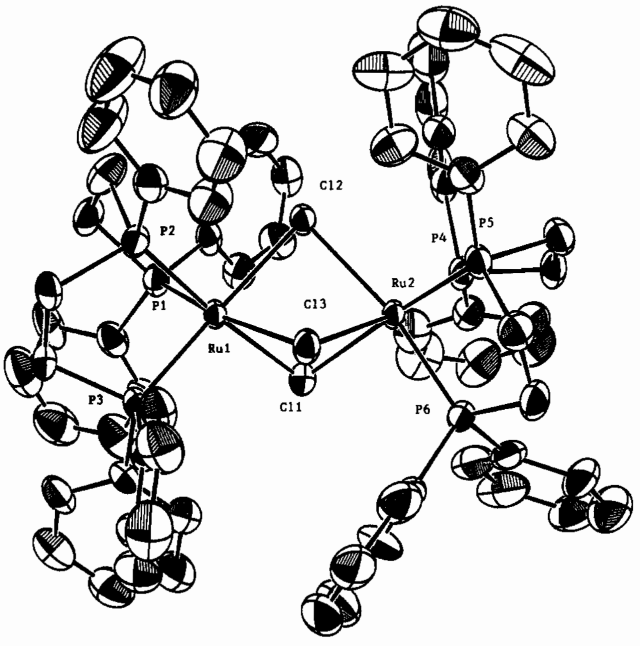

**Figure 1.** ORTEP drawing of the complex cation in the compound *ec*-[$Ru_2(\mu\text{-}Cl)_3(ETP)_2$]($CF_3SO_3$) (**8a**).

---

[13] Jiang, Q.; Rüegger, H.; Venanzi, L. M. Unpublished observation.

**Table II.** Selected Bond Lengths (Å) and Angles (deg) for $[Ru_2(\mu\text{-}Cl)_3(L_3)_2]Y$ ($L_3$ = ETP, Y = $CF_3SO_3$ (**8a**) and $L_3$ = TRIPHOS, Y = $BPh_4$, (**11**))

| $L_3$ = ETP, Y = $CF_3SO_3$ (**8a**) | | | | $L_3$ = TRIPHOS, Y = $[BPh_4]$ (**11**)[2b] |
|---|---|---|---|---|
| | | Bond Lengths | | |
| Ru(1)–Ru(2) | 3.343 (1) | | | 3.455 (1) |
| Ru(1)–P(1)t | 2.284 (2) | Ru(2)–P(6)$_t$ | 2.291 (2) | 2.296 (3) |
| Ru(1)–P(3)$_t$ | 2.266(2) | Ru(2)–P(4)$_t$ | 2.268 (2) | 2.310 (3) |
| Ru(1)–P(2)$_c$ | 2.251(2) | Ru(2)–P(5)$_c$ | 2.252(2) | 2.308(3) |
| Ru(1)–Cl(1)[a] | 2.509(2) | Ru(2)–Cl(1)[a] | 2.509(2) | 2.500(3) |
| Ru(1)–Cl(2)[b] | 2.490(2) | Ru(2)–Cl(3)[b] | 2.478(2) | 2.488(3) |
| Ru(1)–Cl(3)[b] | 2.478(2) | Ru(2)–Cl(2)[b] | 2.490(2) | 2.494(3) |
| | | Bond Angles | | |
| Ru(1)–Cl(1)–Ru(2) | 83.42(5) | | | |
| Ru(1)–Cl(2)–Ru(2) | 84.66(5) | | | 87.8(1) |
| Ru(1)–Cl(3)–Ru(2) | 84.74(5) | | | |
| Cl(1)–Ru(1)–Cl(2) | 80.35(6) | Cl(1)–Ru(2)–Cl(2) | 80.14(5) | 78.0(1) |
| Cl(1)–Ru(1)–Cl(3) | 79.77(5) | Cl(1)–Ru(2)–Cl(3) | 79.96(6) | |
| Cl(2)–Ru(1)–Cl(3) | 79.74(5) | Cl(2)–Ru(2)–Cl(3) | 79.51(5) | 75.5(1) |
| P(1)$_t$–Ru(1)–P(2)$_c$ | 83.72(7) | P(5)$_c$–Ru(2)–P(6)$_t$ | 82.67(7) | 85.5(1) |
| P(2)$_c$–Ru(1)–P(3)$_t$ | 84.35(7) | P(4)$_t$–Ru(2)–P(5)$_c$ | 83.73(7) | 88.6(1) |
| P(1)$_t$–Ru(1)–P(3)$_t$ | 94.82(7) | P(4)$_t$–Ru(2)–P(6)$_t$ | 96.27(7) | 90.8(1) |
| Cl(1)–Ru(1)–P(1)$_t$ | 92.71(6) | Cl(1)–Ru(2)–P(6)$_t$ | 93.62(6) | 97.3(1) |
| Cl(1)–Ru(1)–P(3)$_t$ | 101.63(6) | Cl(1)–Ru(2)–P(4)$_t$ | 101.98(6) | 97.5(1) |
| Cl(2)–Ru(1)–P(1)$_t$ | 90.91(6) | Cl(3)–Ru(2)–P(6)$_t$ | 90.86(6) | 95.7(1) |
| Cl(2)–Ru(1)–P(2)$_c$ | 94.01(6) | Cl(3)–Ru(2)–P(5)$_c$ | 94.77(6) | 96.7(1) |
| Cl(3)–Ru(1)–P(3)$_t$ | 94.80(6) | Cl(2)–Ru(2)–P(4)$_t$ | 93.57(6) | 95.8(1) |
| Cl(3)–Ru(1)–P(2)$_c$ | 102.90(6) | Cl(2)–Ru(2)–P(5)$_c$ | 102.69(6) | 99.3(1) |
| Cl(1)–Ru(1)–P(2)$_c$ | 173.31(6) | Cl(1)–Ru(2)–P(5)$_c$ | 173.54(6) | 175.2(1) |
| Cl(2)–Ru(1)–P(3)$_t$ | 173.83(6) | Cl(3)–Ru(2)–P(4)$_t$ | 172.45(6) | 171.9(1) |
| Cl(3)–Ru(1)–P(1)$_t$ | 168.82(6) | Cl(2)–Ru(2)–P(6)$_t$ | 169.27(6) | 170.1(1) |

[a] Cl trans to $P_c$. [b] Cl trans to $P_t$.

**Table III.** Selected Bond Lengths (Å) and Angles (deg) for Several Cations of the Type $[Ru_2(\mu\text{-}Cl)_3(PR_3)_6]^+$

| complex | Ru–Ru | Ru–P | Ru–Cl | P–Ru–P | Ru–Cl–Ru | Cl–Ru–Cl | ref |
|---|---|---|---|---|---|---|---|
| $[Ru_2(\mu\text{-}Cl)_3(ETP)_2](CF_3SO_3)$ | 3.343(1) | 2.277(9)[a]<br>2.251(2)[b] | 2.484(7)[c]<br>2.509(2)[d] | 96(1)[e]<br>83.6(7)[f] | 84.3(7) | 79.9(3) | this work |
| $[Ru_2(\mu\text{-}Cl)_3(TRIPHOS)_2][BPh_4]$ | 3.455(1) | 2.305(8) | 2.494(6) | 88(3) | 87.8(8) | 77(1) | 2b |
| $[Ru_2(\mu\text{-}Cl)_2(PMe_3)_6][BF_4]$ | 3.275(3) | 2.253(4) | 2.48(1) | 95.4(3) | 82.8(6) | 80.8(5) | 12c |
| $[Ru_2(\mu\text{-}Cl)_2(PMe_2Ph)_6][PF_6]$ | 3.39(1) | 2.290(9) | 2.49(2) | 95(3) | 86(1) | 79(1) | 25 |
| $[Ru_2(\mu\text{-}Cl)_3(PEt_2Ph)_6][RuCl_3(PEt_2Ph)_3]$ | 3.443(4) | 2.318(4) | 2.48(1) | 96(1) | 87.9(4) | 77.1(6) | 26 |
| $[Ru_2(\mu\text{-}Cl)_3(PBu_3)_6][BPh_4]$ | 3.402(1) | 2.30(1) | 2.481(9) | 97(1) | 86.7(4) | 78.0(8) | 12b |
| $[Ru_2(\mu\text{-}Cl)_3(PBu_3)_6][RuCl_4(PBu_3)_2]$ | 3.395(1) | 2.30(1) | 2.48(1) | 96.0(5) | 86.0(5) | 78(1) | 12b |

[a] Ru–$P_t$. [b] Ru–$P_c$. [c] Cl trans to $P_t$. [d] Cl *trans* to $P_c$. [e] $P_t$–Ru–$P_t$. [f] $P_c$–Ru–$P_t$. Esd on the mean has been calculated from: $\sigma = [\sum(X_i - \bar{X})^2/(N-1)]^{1/2}$ where $N$ = number of observations.

The observation that the Ru–$P_c$ distances (2.251(2) (average) Å) are shorter than the corresponding Ru–$P_t$ values (2.277(8) (average) Å) is a recurrent feature of the structural chemistry of chainlike terdentate ligands. This must be caused by the different nature of $P_c$ and $P_t$ atoms, but the available data do not allow a reliable interpretation in terms of either steric or electronic effects, both of them being compatible with the observations.

Probably connected with the differences in the above parameters are the Ru–Cl bond lengths, which also fall into two groups, i.e., those in a *trans*-position to $P_c$ (2.509(2) (average) Å) and those in *trans*-position to $P_t$ (2.484(2) (average) Å). These are in agreement with the expected higher *trans*-influence[14] of the shorter Ru–$P_c$ bonds.

Finally, the Ru–Ru distance in **8a** (3.343(1) Å) is significantly shorter than that in **11** (3.455(1) Å) which is reflected in the smaller Ru–Cl–Ru angles (84.3(7)° (average)) in **8a** than in **11** (87.8° (average)).

The geometric features of the other known trichloro-bridged ruthenium(II) complexes are summarized in Table III.

As can be seen there, the Ru–Ru distances in the compounds containing monodentate ligands range from 3.28 to 3.44 Å while in the TRIPHOS complex **11** this distance is 3.45 Å, the ETP complex **8a** falling in the middle of this range.

**Solid-State NMR Studies.** The presence of only the *ec*-isomer of the cation in the single crystals of **5a** raises the question whether the solids **5** obtained from reactions 1–3 are single isomeric species or mixtures of **5a** and **5b**. For this purpose the $^{31}P$(MAS) spectrum of one of the solids obtained as described for **5** in the Experimental Section was recorded. The spectrum showed broad resonances assignable to the central and terminal phosphine atoms of the coordinated ETP. These broad features are indicative of amorphous regions which could be accounted for by assuming that they originate from the coprecipitation of both isomeric forms of **5**.

Repeating the same experiment with a sample obtained by slow crystallization produced a solid-state $^{31}P$-NMR spectrum exhibiting a total of 12 well-resolved resonance lines. It had been shown earlier[15] that two-dimensional spin-diffusion experiments, which are sensitive to internuclear distances, can be extremely valuble for the interpretation of such complex spectra. Thus, for a dimeric complex like $[Ru_2(\mu\text{-}Cl)_3(ETP)_2]^+$, four types of interaction may be expected: (i) strong between the three phosphorus spins in each ETP moiety, as these atoms are approximately 3.2 Å apart; (ii) medium to weak between the phosphorus atoms of two ETP ligands within the same dimeric unit, where the relevant separations are in the range of ca. 6–7

---

[14] Appleton, T. G.; Clark, H. C.; Manzer, L. E. *Coord. Chem. Rev.* **1973**, *10*, 335.

[15] Blumer, R. E.; Lianza, F.; Pregosin, P. S.; Rüegger, H; Togni, A. *Inorg. Chem.*, in press.

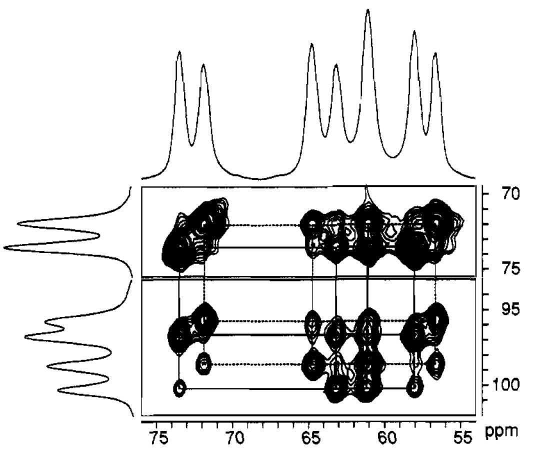

**Figure 2.** Sections of the two-dimensional $^{31}P$ solid-state spin diffusion spectrum for **5** (162 MHz, $\nu_{rot}$ = 12 KHz, $T_{mix}$ = 0.5 s). Parts of the conventional CP-MAS spectrum are plotted as projections, lower left and top for the central and terminal phosphorus resonances, respectively. The two crystallographically independent molecules are indicated with solid and dotted lines, respectively.

Å; (iii) weak between neighboring cations, e.g. where two crystallographically independent molecules are present in the unit cell (based on the crystal structure of **8a** the closest distances between $^{31}P$ spins of neighboring cations are expected to be in the range of ca. 6–8 Å); (iv) absent between different crystallites or phases.

The cross-peak regions in the experimetal spectrum obtained for [Ru$_2$($\mu$-Cl)$_3$(ETP)$_2$]Cl (**5**) is shown in Figure 2.

Four individual ETP ligands having in each case three inequivalent phosphorus atoms are readily recognized from the strongest peaks (type i). These four ligands can be paired, thus establishing the presence of two independent dimers, by considering also the weaker interactions of type ii. Interactions of type iii between the two cations are also clearly indicated, thus excluding the posibility of having two crystalline forms.

Therefore, it can be concluded that "RuCl$_2$(ETP)" is present in the crystal in the form of dimers, presumably of the type [Ru$_2$($\mu$-Cl)$_3$ETP)$_2$]Cl, and that there are two crystallographically independent molecules in the unit cell. However, on the basis of this experiment, one cannot decide whether both isomeric cations are present in the same unit cell, which is of rare occurrence, or whether the single isomer present corresponds to the eclipsed or staggered form as one also expectes for the "symmetrical" *ec*-form six different phosphorus environments in the solid state. In this respect, it should be noted that the X-ray structure analysis of *ec*-[Ru$_2$($\mu$-Cl)$_3$(ETP)$_2$](CF$_3$SO$_3$) (**8a**), mentioned earlier, indeed shows six different coordination sites for the two terdentate phosphine ligands. As expected, the $^{31}P$ spectrum of the corresponding bulk material showed six distinguishable resonances and no significant amount of a second isomer.

Furthermore, when the single crystals of **8a** taken from the batch which had been used for the X-ray diffration work were dissolved in CDCl$_3$ and the $^{31}P$-NMR spectra of the solutions recorded without delay, the presence of both **8a** and **8b**, in the usual ratio, was observed.

In conclusion, the precipitates obtained by reactions 1–3 should be formulated as a mixture of the isomeric pair *ec*-[Ru$_2$($\mu$-Cl)$_3$(ETP)$_2$]Cl (**5a**) and *st*-[Ru$_2$($\mu$-Cl)$_3$(ETP)$_2$]Cl (**5b**). However, slow crystallization leads to the formation of a single isomeric form. Although the above data do not allow a structural assignment, this is likely to be the eclipsed isomer **5a**, based on the information obtained for the single crystal isomer *ec*-[Ru$_2$($\mu$-Cl)$_3$(ETP)$_2$](CF$_3$SO$_3$) (**8a**).

**Solution Behavior and Reactivity of [Ru$_2$($\mu$-Cl)$_3$(ETP)$_2$]$^+$.** As shown in Scheme I, when the isomeric pair **5a** and **5b** is dissolved in acetonitrile, new species are formed. Thus the $^{31}P$-NMR spectrum of an acetonitrile solution of **5** shows the presence of three compounds which are in dynamic equilibrium with each other.

**Scheme I**

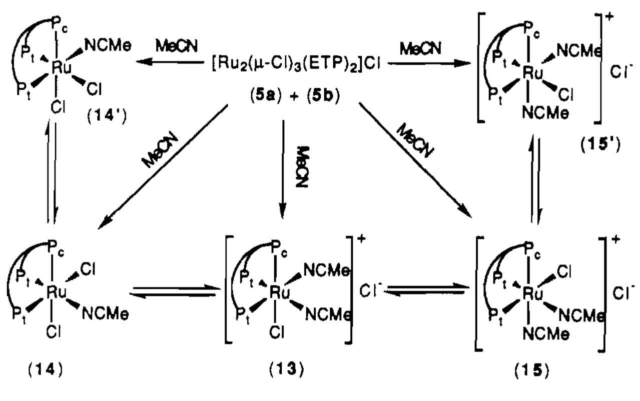

At 25 °C, in CD$_3$CN solution, the major species **13** (ca. 63%) gives a spectrum consisting of a doublet ($\delta$(P) = 58.3 ppm, $J$(P,P) = 18.0 Hz) and a triplet ($\delta$(P) = 100.6 ppm, $J$(P,P) = 18.0 Hz). The second species **14** (ca. 35%), is charaterized by a sharp triplet at $\delta$(P) = 102.0 ppm with $J$(P,P) = 18.7 Hz and a broad resonance at $\delta$(P) = 61.2 ppm. The third species **15** (ca. 2%) gives rise to broad resonances centered at $\delta$(P) = ca. 99.3 ppm and $\delta$(P) = ca. 64.5 ppm. At lower temperatures, e.g. at 0 °C, a typical ABX pattern is observed for this compound.

Complex **13** is assigned to the structure [RuCl(MeCN)$_2$(ETP)]-Cl, with Cl *trans* to the central phosphorus atom, P$_c$, and two molecules of MeCN *trans* to the terminal phosphorus atoms, P$_t$. This assignment is supported by the observation that the single species, produced by the addition of 1 equiv of [PPh$_4$]Cl to a CD$_3$CN solution of [Ru(MeCN)$_3$(ETP)](CF$_3$SO$_3$) (**3**), has a $^{31}P$-NMR spectrum identical to that of the major component of the above solution.

As is apparent from their $^{31}P$-NMR spectra, both **14** and **15** have lower symmetries and, therefore, one of them could be the asymmetrical uncharged dichloro–monosolvento complex and the other the unsymmetrical monochloro–disolvento cation, which is isomeric with **13**. Confirmation of these assignments was obtained from the chloride-dependence of the ratio **13**:**14**:**15**. Thus, in CDCl$_3$/MeCN (8/1), this ratio was ca. 100:12:<0.5 for [Ru$_2$($\mu$-Cl)$_3$(ETP)$_2$][BPh$_4$], ca. 100:29:1 for [Ru$_2$($\mu$-Cl)$_3$(ETP)$_2$]Cl, and ca. 100:37:<0.5 for a mixture of [Ru$_2$($\mu$-Cl)$_3$(ETP)$_2$]Cl and 1 equiv of [PPh$_4$]Cl. Furthermore, the molar conductance of [Ru$_2$($\mu$-Cl)$_3$(ETP)$_2$]Cl (**5**), in the above solvent mixture, was $\Lambda_M$ = 18 ohm$^{-1}$ cm$^2$ mol$^{-1}$, and was lower than the corresponding value for [PPh$_4$]Cl in same medium ($\Lambda_M$ = 38 ohm$^{-1}$ cm$^2$ mol$^{-1}$), indicating that the above solution contains also some uncharged species. Thus, **14** is the unsymmetrical form of the dichloromonoacetonitrile complex [RuCl$_2$(MeCN)(ETP)], and **15** is assigned to the structure [RuCl(MeCN)$_2$(ETP)]Cl, isomeric with **13**, with Cl *trans* to one of the terminal phosphorus atoms. In agreement with the above conclusions, a MeCN solution of **5**, which contains complexes **13**–**15** in a ratio of 100:56:2, shows a molar conductance of 102 ohm$^{-1}$ cm$^2$ mol$^{-1}$, while [Ph$_4$P]Cl gives a value of 123 ohm$^{-1}$ cm$^2$ mol$^{-1}$.

The acetonitrile-containing species shown in Scheme I are in equilibrium with each other. Furthermore, these equilibria are temperature-dependent and the $^{31}P$-NMR data obtained are summarized in Table I.

The complex [RuCl$_2$(Py)(ETP)] (**16**), was obtained by dissolving the binuclear complex **5** in CH$_2$Cl$_2$/pyridine. This complex was charaterized by elemental analysis and IR and one- and two-dimensional $^1H$-, $^{13}C$-, and $^{31}P$-NMR spectroscopy. Thus, the IR spectrum (RbI) gives infrared absorption bands assignable to terminal Ru–Cl stretching vibrations $\nu$(Ru–Cl)$_{asym}$ at 274 cm$^{-1}$ and $\nu$(Ru–Cl)$_{sym}$ at 244 cm$^{-1}$. As the $^{31}P$-NMR spectrum of **16**, in CDCl$_3$ solution, shows an AMX splitting pattern, it is deduced that (a) the ETP ligand is coordinated in a facial mode and (b) pyridine is in *trans*-position to a terminal phosphorus atom as shown in eq 4.

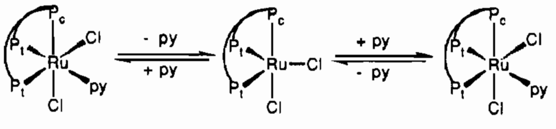

(4)

16 16'

It should be noted that no positional isomer having pyridine in *trans*-position to the central phosphorus atom is present in solution. This is in agreement with the observation that the acetonitrile complexes **13–15** also show a marked preference for the isomers in which chloride is in a *trans*-position to $P_c$. However, complex **16** is fluxional, as shown by two-dimensional $^1H$ exchange spectroscopy; i.e., pyridine exchange occurs whereby this ligand moves from its original position to one in *trans*-position to the other terminal phosphorus atom. This represents an exchange between two possible enantiomers. However, this exchange involves also free pyridine. Thus, one envisages equilibria of the type shown in eq 4.

As mentioned earlier, no ETP-containing ruthenium *tri*solvento complexes appear to have been prepared. The reaction of the isomeric mixture **5** with an excess of $AgCF_3SO_3$, in MeCN, led to the formation of one product of composition $[Ru(MeCN)_3(ETP)](CF_3SO_3)_2$ (**3**), as indicated by its microanalysis and its $^{31}P$(MAS)-NMR spectrum which consisted of three sharp resonances at $\delta(P) = 96, 63$, and 59 ppm, respectively, with broad features at their bases. While these three resonances arise from the inequivalence of the P atoms in solid state, the broad base is attributed[16] to ruthenium satellites with $J(Ru,P) \simeq 160$ Hz. The absence of a large P,P coupling is consistent with a facial coordination of ETP. However, the $^{31}P$-NMR spectrum of this compound, recorded in $CDCl_3$, showed the presence of two complexes, each having a spectrum characteristic of an $AX_2$ spin system, one of them with a triplet at $\delta(P) = 96.7$ ($J(P,P) = 17.8$ Hz) and a doublet at $\delta(P) = 60.2$ ppm and the other with a triplet at $\delta(P) = 104.3$ ppm with $J(P,P) = 20.1$ Hz and a doublet at $\delta(P) = 58.1$ ppm. The latter resonances disappeared when a small amount of acetonitrile was added to the $CDCl_3$ solution. Thus, the former set of signals is assigned to the *tri*solvento complex $[Ru(MeCN)_3(ETP)](CF_3SO_3)_2$ (**3**) and the latter to the *mono*-triflate *bis*(acetonitrile) complex $[Ru(CF_3SO_3)(MeCN)_2(ETP)](CF_3SO_3)$ (**7**).

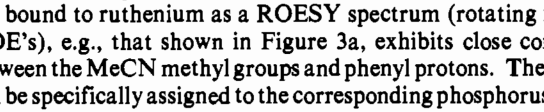

(5)

3 7

One- and two-dimensional $^1H$-NMR spectroscopy is fully consistent with two complexes formulated as **3** and **7**, respectively. Thus, for compound **3**, two types of acetonitrile are found at $\delta(H) = 2.89$ and 1.85 ppm in the ratio 1:2. These acetonitrile molecules are bound to ruthenium as a ROESY spectrum (rotating frame NOE's), e.g., that shown in Figure 3a, exhibits close contacts between the MeCN methyl groups and phenyl protons. The latter can be specifically assigned to the corresponding phosphorus spins by means of a P,H correlation. Furthermore, the presences of only two types of MeCN in this complex proves unambiguously the facial coordination of the terdentate phosphine ligand. In addition to the resonances assigned to **3**, two other types of MeCN (also in the ratio 1:2) are visible at $\delta(H) = 2.01$ and 1.72 ppm, respectively. While the former is assigned to free MeCN as (1) it lacks closeness to phenyl protons and (2) the signal intensity grows when more nitrile is added to the solution, the latter is assigned to the symmetrical *bis*(acetonitrile) complex **7**.

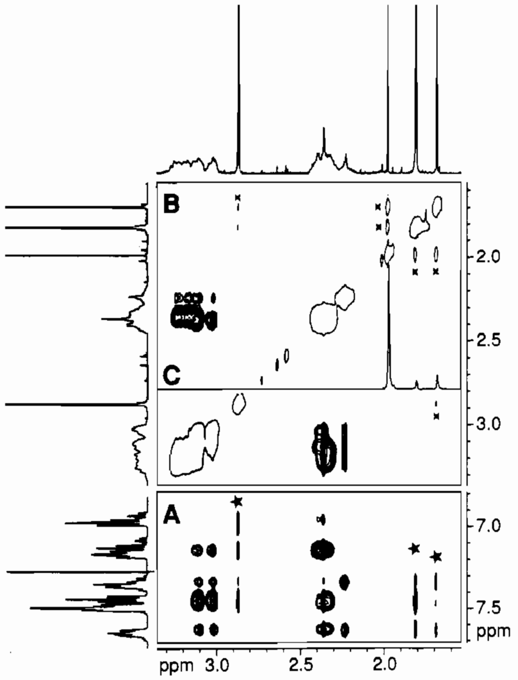

**Figure 3.** Parts of the 500.13-MHz ROESY spectrum (400-ms CW spinlock with $\gamma B_1/2\pi \approx 7$ kHz) of the solvento complexes $[Ru(MeCN)_3(ETP)](CF_3SO_3)_2$ (**3**) and $[Ru(CF_3SO_3)(MeCN)_2(ETP)](CF_3SO_3)$ (**7**) in $CDCl_3$ solution, showing (A) the spatial closeness of coordinated acetonitrile to phenyl protons (★), (B) the exchange between various types of acetonitrile (×), and (C) a trace at the position of free acetonitrile exhibiting preferential exchange with positions trans to terminal phosphorus atoms $P_t$ in **7** and **3**.

This *bis*(solvento) complex can be prepared by heating $[Ru(MeCN)_3(ETP)](CF_3SO_3)_2$ (**3**) at ca 100 °C, under high vacuum, for 2 days. The formulation of complex **7** has also been confirmed by its $^{19}F$-NMR spectrum in $CDCl_3$ solution, which shows two resonance signals at $\delta(F) = -78.24$ and $-78.56$ ppm, respectively. The latter resonance shows a small NOE enhancement when the protons are irradiated and, therefore, is assigned to the coordinated triflate. These $^{19}F$ chemical shift values can be compared with that of the TRIPHOS complex $[Ru(MeCN)_3(TRIPHOS)](CF_3SO_3)_2$, (**2**), which gave only one singlet at $\delta(F) = -78.52$ ppm ($CD_2Cl_2$).[2a]

The nitrile-containing complexes show dynamic behavior in solution involving **3**, **7**, and free acetonitrile. Part of the ROESY spectrum of a solution containing these species is shown in Figure 3. As can be seen qualitatively there, free acetonitrile exchanges preferentially with that bound to complex **7** and, to a lesser extent, with that in the *trans*-position to the terminal phosphorus atoms in **3**.

**X-ray Crystal Structure of $[Ru(MeCN)_3(ETP)](CF_3SO_3)_2$ (3).** The crystals of **3** contain discrete $[Ru(MeCN)_3(ETP)]^{2+}$ cations and disordered $CF_3SO_3^-$ anions, separated by normal van der Waals distances. The lower accuracy of the structure determination (see Experimental Section) is a consequence of this disorder. An ORTEP drawing of the cation is shown in Figure 4, and a selection of interatomic distances and bond angles is given in Table IV.

The coordination at the ruthenium atom is distorted octahedral, and the P donors of the ETP ligand occupy mutually *cis*-positions. The P–Ru–P, P–Ru–N, and N–Ru–N angles range from 84 to 98° for *cis*-positions and from 172 to 178° for *trans*-positions. The Ru–P distances also differ: that between ruthenium and the central phosphorus atom $P_c$ (2.261(6) Å) is shorter than those *trans* to the two terminal phosphorus atoms (2.312(6) (average) Å), as found in the binuclear compound **8a**. The Ru–N distances are equal within the standard deviations which, however, are

---

(16) Eichele, K.; Wasylishen, R. E.; Corrigan, J. F.; Doherty, S.; Sun, Y.; Carty, A. J. *Inorg. Chem.* **1993**, *32*, 121.

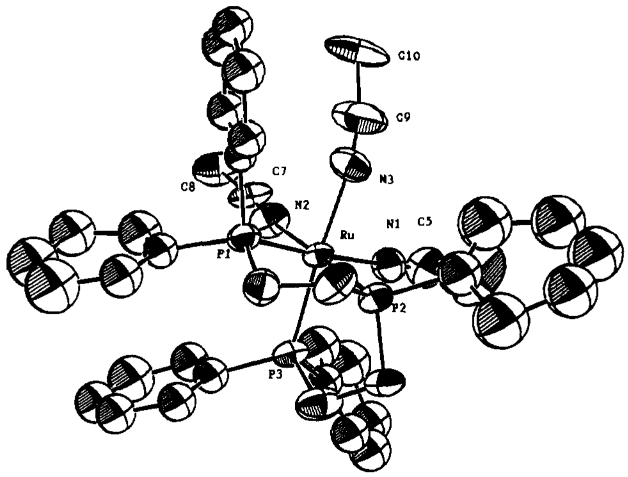

**Figure 4.** ORTEP drawing of the complex cation in [Ru(MeCN)$_3$(ETP)]-(CF$_3$SO$_3$)$_2$ (3).

**Table IV.** Selected Bond Lengths (Å) and Angles (deg) for the Complex Cation [Ru(MeCN)$_3$(ETP)]$^{2+}$ (3)

| | | | |
|---|---|---|---|
| | Bond Lengths | | |
| Ru–P(1)$_t$ | 2.314(6) | Ru–N(1) | 2.10(2) |
| Ru–P(2)$_c$ | 2.261(6) | Ru–N(2) | 2.13(2) |
| Ru–P(3)$_t$ | 2.309(6) | Ru–N(3) | 2.13(2) |
| | Bond Angles | | |
| P(1)$_t$–Ru–P(2)$_c$ | 84.5(2) | P(1)$_t$–Ru–N(2) | 97.1(6) |
| P(2)$_c$–Ru–P(3)$_t$ | 84.0(2) | P(1)$_t$–Ru–N(3) | 90.9(6) |
| P(1)$_t$–Ru–P(3)$_t$ | 95.3(2) | P(2)$_c$–Ru–N(1) | 90.7(6) |
| N(1)–Ru–N(2) | 87.7(8) | P(2)$_c$–Ru–N(3) | 97.6(6) |
| N(2)–Ru–N(3) | 83.9(8) | P(3)$_t$–Ru–N(1) | 89.9(5) |
| N(1)–Ru–N(3) | 84.0(8) | P(3)$_t$–Ru–N(2) | 94.3(6) |
| | | P(1)$_t$–Ru–N(1) | 172.5(6) |
| | | P(2)$_c$–Ru–N(2) | 177.7(6) |
| | | P(3)$_t$–Ru–N(3) | 173.7(6) |

large and, therefore, may mask even a significant difference in Ru–N bond distances. Interestingly, the Ru–N$_2$ bond, with a numerically larger value, is in the *trans*-position to the Ru–P$_c$ bond, which is the shortest.

**TTP Complexes.** The reaction of *cis*-[RuCl$_2$(DMSO)$_4$] and TTP in acetone, THF, or toluene gives a product of composition *fac*-[RuCl$_2$(TTP)] (6), which is sparingly soluble in common organic solvents. It is, however, soluble in solvent mixtures such as CH$_2$Cl$_2$ (or CHCl$_3$) and MeCN. The far-infrared spectrum of the recrystallized product, which is monomeric in the solid state (see later), shows absorptions at 357, 290, and 259 cm$^{-1}$, and the latter two are likely to be due to $\nu$(Ru–Cl)$_{asym}$ and $\nu$(Ru–Cl)$_{sym}$, respectively. Similar low Ru-Cl stretching absorptions ($\nu$(Ru–Cl): 273, 254 cm$^{-1}$) have been observed for *cis*-[RuCl$_2$(DCPE)$_2$] (DCPE = 1,2-bis(dicyclohexylphosphino)ethane).[17]

The $^{31}$P-NMR spectrum of 6, in the solvent mixture CDCl$_3$/MeCN (ca. 8:1), shows an AMX pattern giving resonances with $\delta$(P) values at $\delta$(P) = 28.2 (dd, $J$(P,P) = 39.6, 27.7 Hz), 25.8 (dd, J(P,P) = 46.8, 27.7 Hz), and 18.2 ppm (dd, $J$(P,P) = 46.8, 39.6 Hz), respectively, each of them arising from one of the three non-equivalent phosphorus atoms. The values of the coupling constants between the phosphorus atoms indicate a facial coordination of TTP. In CDCl$_3$/MeCN (8:1) and in pure MeCN, molar conductivity measurement gave values of 33 and 115 ohm$^{-1}$ cm$^2$ mol$^{-1}$, respectively, comparable with the corresponding values (38 and 123 $\Omega^{-1}$ cm$^2$ mol$^{-1}$) for [PPh$_4$]Cl in the same solvents.

Although the appropriate resonances for bound MeCN are not observed at room temperature, probably due to fast exchange with free MeCN, which is present in large excess, 17 is formulated as a *bis*(acetonitrile) cationic complex, *fac*-[RuCl(MeCN)$_2$(TTP)]Cl. Obviously, this is not the only structure possible on the basis of the spectral data obtained, but it is the most likely if one takes into account of the conductivity measurements.

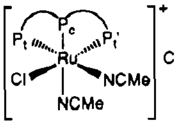

17

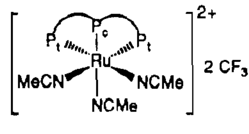

4

The reaction of *fac*-[RuCl$_2$(TTP)] (6) with 2 equiv of AgCF$_3$SO$_3$ in acetonitrile gave, after normal workup, the TTP *tri*solvento complex *fac*-[Ru(MeCN)$_3$(TTP)](CF$_3$SO$_3$)$_2$ (4), which was characterized by microanalysis as well as by IR and $^{31}$P-NMR spectroscopy. The $^{31}$P{$^1$H}-NMR spectrum of this compound, in CDCl$_3$, showed an AX$_2$ splitting pattern (see Table I), consistent with the expected *fac*-octahedral structure. This was confirmed by the $^1$H-NMR (CDCl$_3$) of 4, which showed only two resonance signals assignable to the coordinated acetonitrile ($\delta$(H) = 2.19 and 2.00 ppm), whereas, on the basis of the X-ray crystal structure of the compound *mer, cis, anti*-[RuH$_2$(N$_2$)(CyTTP)] (CyTTP = PhP(CH$_2$CH$_2$CH$_2$PCy$_2$)$_2$) (18),[18] the hypothetical *mer*-isomer of 4, i.e. 19, containg meridionally coordinated TTP, should give rise to three resonance signals for the bound MeCN due to the orientation of the phenyl substituent on P$_c$ which renders the two apical MeCN different from each other:

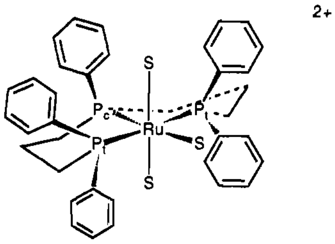

(S = MeCN)

19

Finally, it is worth noting that, in the dicationic complex *fac*-[Ru(MeCN)$_3$(TTP)]$^{2+}$ (4), the two P$_t$ atoms of this ligand occupy mutually *cis*-positions although several complexes, in addition to 18, are known in which a meridional coordination of this ligand is found.[9,10]

**X-ray Crystal Structure of *fac*-[RuCl$_2$(TTP)] (6).** The crystal contains discrete molecules of *fac*-[RuCl$_2$(TTP)] (6), separated by normal van der Waals distances. Thus it is not dimeric or polymeric as postulated earlier on the basis of its low solubility.[10d] An ORTEP drawing of the molecule is shown in Figure 5. A selection of relevant interatomic distances and angles is shown in Table V.

The ruthenium atom is coordinated to the two chlorine atoms and the three phosphorus atoms of TTP. The coordination geometry at the metal center is intermediate between that of a trigonal bipyramid and a square pyramid. If one describes the distortion starting from the square pyramidal model, using the Ru–P$_2$ vector as the molecular axis, the main deviations from ideal geometry are the angles Cl(2)–Ru–P(2)$_c$ and P(1)$_t$–Ru–P(3)$_t$, which, instead of being ca. 90°, are 122.89(9) and 100.41(8)°, respectively. Distortions calculated on the basis of a trigonal bipyramidal structure are somewhat larger.

The Ru–P$_c$ distance (2.198(2) Å) is shorter than the Ru–P$_t$ distances (2.271(2) (average) Å), as is the case for the ETP complexes 8a and 3 described earlier. Furthermore, the Ru–P$_c$ distance in 6 is shorter than the corresponding distance in 8a (2.252(2) Å) while the Ru–P$_t$ distances in 6 (2.271(2) (average) Å) do not differ significantly from the corresponding distances

---

(17) Mezzetti, A.; Zotto, A. D.; Rigo, P. *J Chem. Soc., Dalton Trans.* **1990**, 2515.

(18) Jia, G. ; Meek. D. W., Gallucci, J. C. *Inorg. Chem.* **1991**, *30*, 403.

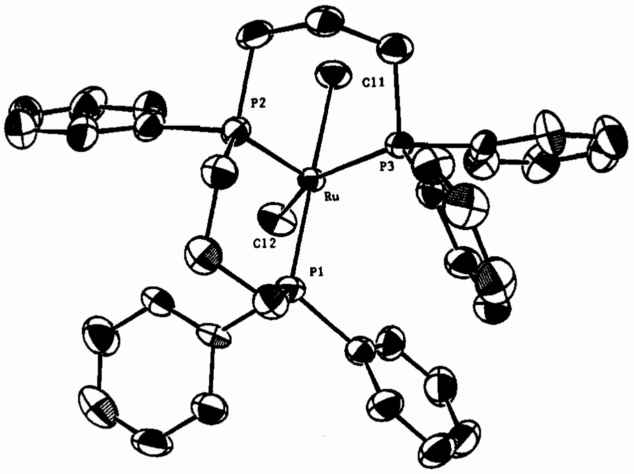

**Figure 5.** ORTEP drawing of the compound *fac*-$[RuCl_2(TTP)]$ (**6**).

**Table V.** Selected Bond Lengths (Å) and Angles (deg) for *fac*-$[RuCl_2(TTP)]$ (**6**) and $[RuCl_2(CyTTP)]\cdot 2DMSO$ (**20**)[10f]

| | *fac*-$[RuCl_2(TPP)]$ (**6**) | $[RuCl_2(CyTTP)]\cdot$ 2DMSO (**20**) |
|---|---|---|
| | Bond Lengths | |
| Ru–Cl(1) | 2.439(2) | 2.455(1) |
| Ru–Cl(2) | 2.394(2) | 2.406(2) |
| Ru–$P(1)_t$ | 2.280(2) | 2.306(1) |
| Ru–$P(2)_c$ | 2.198(2) | 2.212(2) |
| Ru–$P(3)_t$ | 2.261(2) | 2.276(2) |
| | Bond Angles | |
| Cl(1)–Ru–Cl(2) | 85.16(8) | 83.32(6) |
| Cl(1)–Ru–$P(1)_t$ | 172.48(9) | 167.95(5) |
| Cl(1)–Ru–$P(2)_c$ | 93.72(9) | 90.19(5) |
| Cl(1)–Ru–$P(3)_t$ | 84.91(8) | 88.40(5) |
| Cl(2)–Ru–$P(1)_t$ | 87.63(8) | 86.86(6) |
| Cl(2)–Ru–$P(2)_c$ | 122.89(9) | 137.73(7) |
| Cl(2)–Ru–$P(3)_t$ | 150.24(9) | 134.00(7) |
| $P(1)_t$–Ru–$P(2)_c$ | 91.90(8) | 92.60(5) |
| $P(2)_c$–Ru–$P(3)_t$ | 86.72(8) | 87.18(6) |
| $P(1)_t$–Ru–$P(3)_t$ | 100.41(8) | 103.41(5) |

**Table VI.** Experimental Data for the X-ray Diffraction Study of Compounds **8a**$\cdot CH_2Cl_2$, **3**, and **6**

| | **8a**$\cdot CH_2Cl_2$ | **3** | **6** |
|---|---|---|---|
| formula | $C_{70}H_{68}Cl_5F_3O_3$-$P_6Ru_2S$ | $C_{42}H_{42}F_6N_3O_6$-$P_3RuS_2$ | $C_{36}H_{37}Cl_2P_3Ru$ |
| mol wt | 1611.63 | 1056.93 | 734.59 |
| $T$, °C | 23 | 23 | 23 |
| space group | $P\bar{1}$ (No. 2) | $P2_1/n$ (No. 14) | $Cc$ (No. 9) |
| $a$, Å | 12.451(2) | 15.138(4) | 21.861(4) |
| $b$, Å | 17.320(1) | 18.776(6) | 10.175(1) |
| $c$, Å | 18.646(3) | 16.737(3) | 18.710(5) |
| $\alpha$, deg | 75.95(2) | 90 | 90 |
| $\beta$, deg | 70.98(1) | 91.35(2) | 127.98(2) |
| $\gamma$, deg | 71.55(2) | 90 | 90 |
| $V$, Å$^3$ | 3562(2) | 4756(2) | 3280(1) |
| $Z$ | 2 | 4 | 4 |
| $\rho$(calc), g cm$^{-3}$ | 1.502 | 1.476 | 1.487 |
| $\mu$, cm$^{-1}$ | 7.410 | 5.747 | 8.015 |
| $\lambda$, Å | 0.710 69 (graphite monochromated) | | |
| $\theta$ range, deg | $2.5 < \theta < 23.0$ | $2.5 < \theta < 23.5$ | $2.5 < \theta < 25.0$ |
| transm coeff | 0.7366–0.9999 | 0.7372–0.9996 | 0.8395–0.9952 |
| $R^a$ | 0.050 | 0.063 | 0.034 |
| $R_w{}^b$ | 0.062 | 0.094 | 0.040 |

[a] $R = \sum(||F_o| - (1/k)|F_c||)/\sum|F_o|$. [b] $R_w = [\sum w(|F_o| - (1/k)|F_c|)^2/\sum w|F_o|^2]^{1/2}$, where $w = [\sigma^2(F_o)]^{-1}$; $\sigma(F_o) = [\sigma^2(F_o^2) + f^4(F_o^2)]^{1/2}/2F_o$.

in **8a** (2.277(8) (average) Å). As found in complex **8a**, the $P_c$–Ru–$P_t$ bond angles in complex **6** (86.72(8) and 91.90(8)°) are smaller than the $P_t$–Ru–$P_t$ (100.41(8)°) angle. However, the $P_c$-Ru-$P_t$ and $P_t$-Ru-$P_t$ angles in **6** are larger than the corresponding angles in $[Ru(MeCN)_3(ETP)](CF_3SO_3)_2$ (**3**) (84.2(3) (average) and 95.3(2)° (average), respectively).

The two Ru–Cl distances are significantly different (Ru–Cl(1) = 2.439(2) Å; Ru–Cl(2) = 2.394(2) Å), and it is noteworthy that the longer bond is directly in a *trans*-position to a phosphorus donor.

This structure is quite similar to that found by Jia *et al.*[10f] in $[RuCl_2(CyTTP)]\cdot 2DMSO$ (**20**) (CyTTP = $PhP(CH_2CH_2CH_2PCy_2)_2$). The relevant coordination parameters for this structure are also listed in Table V. The most significant differences are (1) the Ru–Cl and Ru–P distances are shorter in **6** than in **20** and (2) the structure of **20** is closer to a trigonal bipyramid than that of **6**. These differences may be associated with the difference in electron-density at the metal center. In general one finds that electron-rich metal centers induce trigonal bipyramidal coordination while a lower electronic charge of the metal center leads to the formation of square pyramidal structures.[19]

Finally, the mononuclear nature of *fac*-$[RuCl_2(TTP)]$ (**6**), as opposed to the normal trichloro-bridged bimetallic structure of cations formed by ETP, **5a** and **5b**, is likely to be caused by the greater van der Waals repulsions which would arise in a TTP complex as the unit "Ru(TTP)" occupies a larger volume than "Ru(ETP)".

## Experimental Section

All syntheses and manipulations involving phosphine ligands and complexes were performed under an inert atmosphere (nitrogen or argon) using standard Schlenk techniques. The solvents used were purchased from Fluka AG and, unless otherwise stated, were used as received. Benzene, toluene, diethyl ether, tetrahydrofuran, hexane, and pentane were distilled from sodium benzophenone ketyl under nitrogen. Acetonitrile was distilled from $CaH_2$ under a nitrogen atmosphere.

The NMR-spectra were measured on Bruker AC 250, AMX 400, and AMX 500 instruments. The chemical shifts are given in $\delta$ (ppm), the positive values denoting a downfield shift relative to the reference. Coupling constants are given in hertz. The $^{31}P$ solid-state NMR spectra were recorded on a Bruker AMX 400 spectrometer using magic-angle spinning (rates between 10 and 15 kHz) and cross-polarization techniques. Two-dimensional spin-diffusion experiments were carried out as previously described.[15] The infrared spectra were recorded on a Perkin-Elmer 883 spectrophotometer as KBr or RbI pellets. The observed range was 4000–200 cm$^{-1}$. Conductivity data were obtained on $10^{-3}$ M nitromethane or acetonitrile solutions, unless otherwise noted, with a Metrohm E527 Konduktometer. The molar conductance $\Lambda_M$ has the unit ohm$^{-1}$ cm$^2$ mol$^{-1}$. The elemental analyses were performed by the Microanalytical Laboratory of, Institute of Organic Chemistry, Swiss Federal Institute of Technology, Zürich, Switzerland. The FAB Mass Spectra were measured on a FISONS/VG-ZAB-VSEQ double-focusing mass spectrometer at 8-kV accelerating voltage by the MS service of the Laboratory of Organic Chemistry, ETH-Zürich. Typically, 50–100 $\mu$g of analyte was dissolved in 1 $\mu$L of mNBA matrix (*m*-nitrobenzylic alcohol) and bombarded with $Cs^+$ ions (35 kV at 2 $\mu$A) on a stainless steel target. The centroided positive spectra were recorded with the VG-OPUS data system (Version 1.7F) from $m/z$ = 2000 to $m/z$ = 50 at a speed of 5 s/decade and a instrument resolution of $m/\Delta m = 2000$, merging four to five scans together.

The complex $[RuCl_2(PPh_3)_3]$ was purchased from Fluka Chemie AG, and $RuCl_3\cdot nH_2O$ was obtained from the Aldrich Chemical Co. The ligand ETP[20] and the complexes *cis*-$[RuCl_2(DMSO)_4]$[21] and $[Ru(MeCN)_3(TRIPHOS)](CF_3SO_3)_2$[2] were prepared as described in the literature, while the phosphine ligand TTP was prepared by starting from $Ph_2PCH_2CH_2CH_2Cl$[22] and reacting it with $PhPLi_2$.[23,24]

**$[Ru_2(\mu\text{-}Cl)_3(ETP)_2]Cl\cdot 2H_2O$ (5).** From $[RuCl_2(PPh_3)_3]$. A 250-mL three-necked flask, fitted with a nitrogen inlet, a reflux condenser, and a dropping addition funnel, was charged with bis(2-(diphenylphosphino)ethyl)phenylphosphine (1.14 g, 2.13 mmol) and benzene (30 mL). A suspension of $[RuCl_2(PPh_3)_3]$ (2.02 g, 2.11 mmol) in benzene (100 mL)

---

(19) Rossi, A. R.; Hoffmann, R. *Inorg. Chem.* **1975**, *14*, 365.
(20) King, R. B.; Kapoor, P. N. *J. Am. Chem. Soc.* **1971**, *97*, 4158.
(21) Evans, I. P.; Spencer, A.; Wilkinson, G. *J. Chem. Soc., Dalton Trans.* **1973**, 204.
(22) Green, L. M.; Meek, D. W. *Polyhedron* **1990**, *9*, 35.
(23) Mazanec, T. J.; Tau, K. D.; Meek, D. W. *Inorg. Chem.* **1980**, *19*, 85.
(24) Arpac, E.; Dahlenburg, L. *Z. Naturforsch.* **1980**, *35b*, 146.
(25) Laing, M.; Pope, L. *Acta Crystallogr., Sect. B: Struct. Crystallogr. Cryst. Chem.* **1976**, *B32*, 1547.
(26) Raspin, K. A.; *J. Chem. Soc., A* **1969**, 461.

**Table VII.** Final Positional and Isotropic Equivalent Displacement Parameters ($B_{iso}$ in Å$^2$) for the Complex *ec*-[$Ru_2(\mu\text{-}Cl)_3(ETP)_2$]($CF_3SO_3$)·$CH_2Cl_2$ (**8a**·$CH_2Cl_2$)[a]

| atom | *x* | *y* | *z* | *B*, Å$^2$ | atom | *x* | *y* | *z* | *B*, Å$^2$ |
|---|---|---|---|---|---|---|---|---|---|
| Ru(1) | 0.83410(4) | 0.14624(3) | 0.25532(3) | 2.15(1) | C(311) | 1.0419(6) | 0.1314(4) | 0.0741(4) | 3.2(2) |
| Ru(2) | 0.76047(4) | 0.33738(3) | 0.29498(3) | 2.26(1) | C(312) | 1.0559(7) | 0.1533(4) | –0.0047(4) | 4.2(2) |
| Cl(1) | 0.6748(1) | 0.27201(9) | 0.22805(9) | 2.95(3) | C(313) | 1.1617(7) | 0.1724(5) | –0.0522(5) | 5.2(2) |
| Cl(2) | 0.7714(1) | 0.20022(9) | 0.37789(8) | 2.77(3) | C(314) | 1.2475(7) | 0.1669(5) | –0.0218(6) | 6.1(3) |
| Cl(3) | 0.9434(1) | 0.25378(9) | 0.21790(8) | 2.73(3) | C(315) | 1.2357(6) | 0.1457(5) | 0.0568(5) | 5.1(2) |
| S | 0.1075(2) | 0.2965(1) | 0.7167(1) | 4.38(5) | C(316) | 1.1334(6) | 0.1291(4) | 0.1048(4) | 4.1(2) |
| P(1) | 0.7062(1) | 0.06460(9) | 0.30478(9) | 2.72(4) | C(321) | 0.8215(5) | 0.1191(4) | 0.0739(3) | 3.2(2) |
| P(2) | 0.9641(1) | 0.0327(1) | 0.29413(9) | 2.79(4) | C(322) | 0.8101(6) | 0.0543(4) | 0.0454(4) | 4.0(2) |
| P(3) | 0.9096(1) | 0.10097(9) | 0.14031(9) | 2.72(4) | C(323) | 0.7482(6) | 0.0716(5) | –0.0063(4) | 5.0(2) |
| P(4) | 0.5976(1) | 0.40132(9) | 0.37907(9) | 2.89(4) | C(324) | 0.6901(7) | 0.1531(6) | –0.0302(5) | 5.8(2) |
| P(5) | 0.8539(1) | 0.39654(9) | 0.34278(9) | 2.80(4) | C(325) | 0.6966(8) | 0.2163(6) | –0.0019(5) | 5.7(2) |
| P(6) | 0.7700(2) | 0.4496(1) | 0.20036(9) | 3.02(4) | C(326) | 0.7648(7) | 0.1999(5) | 0.0514(4) | 4.5(2) |
| F(1) | –0.0397(6) | 0.2239(4) | 0.8233(4) | 10.3(2) | C(411) | 0.4505(6) | 0.4375(4) | 0.3652(4) | 3.7(2) |
| F(2) | –0.1049(6) | 0.3552(5) | 0.7961(4) | 11.4(3) | C(412) | 0.4060(6) | 0.3859(5) | 0.3439(5) | 5.0(2) |
| F(3) | –0.0915(4) | 0.2769(4) | 0.7192(4) | 9.6(2) | C(413) | 0.2912(7) | 0.4125(6) | 0.3387(7) | 7.1(3) |
| O(1) | 0.1523(5) | 0.3036(4) | 0.7745(3) | 6.5(2) | C(414) | 0.2208(8) | 0.4909(6) | 0.3511(6) | 7.1(3) |
| O(2) | 0.1593(6) | 0.2233(4) | 0.6826(4) | 7.6(2) | C(415) | 0.2672(7) | 0.5416(6) | 0.3736(6) | 6.1(3) |
| O(3) | 0.0881(6) | 0.3702(4) | 0.6631(3) | 6.8(2) | C(416) | 0.3768(7) | 0.5181(5) | 0.3786(5) | 5.0(2) |
| C(F) | –0.0382(8) | 0.2880(6) | 0.7651(6) | 6.2(3) | C(421) | 0.5687(6) | 0.3450(4) | 0.4779(4) | 3.5(2) |
| C(1) | 0.7802(6) | –0.0376(4) | 0.3488(4) | 3.8(2) | C(422) | 0.6590(7) | 0.3116(4) | 0.5125(4) | 4.3(2) |
| C(2) | 0.8832(6) | –0.0303(4) | 0.3745(5) | 4.2(2) | C(423) | 0.6417(9) | 0.2720(5) | 0.5902(5) | 6.2(3) |
| C(3) | 0.9654(6) | –0.0131(4) | 0.1595(4) | 3.4(2) | C(424) | 0.526(1) | 0.2685(6) | 0.6314(5) | 6.8(3) |
| C(4) | 1.0381(6) | –0.0343(4) | 0.2184(4) | 3.8(2) | C(425) | 0.4329(8) | 0.3006(5) | 0.5964(5) | 6.4(3) |
| C(5) | 0.6245(6) | 0.4951(4) | 0.3918(4) | 3.7(2) | C(426) | 0.4539(7) | 0.3386(4) | 0.5214(4) | 4.7(2) |
| C(6) | 0.7481(6) | 0.4762(4) | 0.4003(4) | 3.6(2) | C(511) | 0.9492(5) | 0.3434(4) | 0.4050(4) | 3.3(2) |
| C(7) | 0.8604(6) | 0.5075(4) | 0.2130(4) | 4.1(2) | C(512) | 0.9853(6) | 0.2583(5) | 0.4175(5) | 4.6(2) |
| C(8) | 0.9434(6) | 0.4543(4) | 0.2630(4) | 3.7(2) | C(513) | 1.0501(7) | 0.2167(6) | 0.4713(5) | 6.1(3) |
| C(111) | 0.6332(5) | 0.0399(4) | 0.2460(4) | 3.5(2) | C(514) | 1.0744(7) | 0.2618(7) | 0.513(5) | 6.2(3) |
| C(112) | 0.6270(6) | –0.0413(4) | 0.2522(5) | 5.1(2) | C(515) | 1.0441(7) | 0.3455(7) | 0.4983(5) | 6.9(3) |
| C(113) | 0.5645(8) | –0.0534(6) | 0.2052(6) | 7.0(3) | C(516) | 0.9778(7) | 0.3889(5) | 0.4442(5) | 5.2(2) |
| C(114) | 0.5083(8) | 0.0089(6) | 0.1596(5) | 6.9(2) | C(611) | 0.8428(7) | 0.4245(4) | 0.1038(4) | 3.9(2) |
| C(115) | 0.5124(7) | 0.0903(6) | 0.1560(5) | 5.9(2) | C(612) | 0.9638(8) | 0.4078(5) | 0.0777(5) | 5.5(2) |
| C(116) | 0.5778(6) | 0.1028t5) | 0.1986(4) | 3.9(2) | C(613) | 1.0193(8) | 0.3843(5) | 0.0024(5) | 6.0(3) |
| C(121) | 0.5790(5) | 0.1034(4) | 0.3831(4) | 3.1(1) | C(614) | 0.9557(9) | 0.3779(5) | –0.0420(5) | 6.5(3) |
| C(122) | 0.5890(6) | 0.0815(5) | 0.4596(4) | 4.1(2) | C(615) | 0.8343(9) | 0.3978(6) | –0.0166(5) | 6.9(3) |
| C(123) | 0.4959(7) | 0.1136(5) | 0.5176(4) | 4.8(2) | C(616) | 0.7768(8) | 0.4189(5) | 0.0580(4) | 5.7(2) |
| C(124) | 0.3908(6) | 0.1656(4) | 0.5035(4) | 3.9(2) | C(621) | 0.6360(7) | 0.5277(4) | 0.1878(4) | 4.0(2) |
| C(125) | 0.3821(6) | 0.1855(5) | 0.4294(4) | 4.4(2) | C(622) | 0.5405(7) | 0.5026(5) | 0.1877(4) | 4.7(2) |
| C(126) | 0.4762(6) | 0.1538(4) | 0.3700(4) | 3.8(2) | C(623) | 0.4375(8) | 0.5578(6) | 0.1782(5) | 6.5(3) |
| C(211) | 1.0868(6) | 0.0292(4) | 0.3282(4) | 3.6(2) | C(624) | 0.4309(9) | 0.6457(6) | 0.1687(6) | 7.2(3) |
| C(212) | 1.1384(8) | –0.0414(6) | 0.3690(6) | 7.8(3) | C(625) | 0.5251(9) | 0.6701(6) | 0.1644(6) | 7.0(3) |
| C(213) | 1.2386(8) | –0.0433(6) | 0.3971(7) | 8.9(3) | C(626) | 0.6306(8) | 0.6132(5) | 0.1765(5) | 5.8(2) |
| C(214) | 1.2834(7) | 0.0234(6) | 0.3741(5) | 6.3(2) | Cl(1s) | 0.2679(9) | 0.3028(6) | 0.1694(6) | 28.7(4)* |
| C(215) | 1.2139(7) | 0.0927(5) | 0.3318(5) | 5.9(2) | C(1s) | 0.415(2) | 0.337(1) | 0.149(1) | 14.7(6)* |
| C(216) | 1.1362(6) | 0.0975(5) | 0.3088(5) | 4.9(2) | Cl(2s) | 0.404(10 | 0.3935(8) | 0.0635(8) | 38.6(7)* |

[a] Esd's are given in parentheses. The atoms labeled C(*ns*) and Cl(*ns*) are those of the solvent molecule. Atom C(F) is the carbon atom of the triflate counterion. Values marked with an asterisk denote atoms that were refined isotropically. Values for anisotropically refined atoms are given in the form of the isotropic equivalent displacement parameter defined as $(4/3)[a^2B(1,1) + b^2B(2,2) + c^2B(3,3) + ab(\cos\gamma)B(1,2) + ac(\cos\beta)B(1,3) + bc(\cos\alpha)B(2,3)]$.

was added dropwise at ca. 50 °C over 40 min. The resulting red-brown mixture was refluxed for 12 h. The volume of the mixture was reduced to ca. 20 mL under reduced pressure, and petroleum ether (100 mL) was added. The yellow crude product was filtered off and dissolved in ethanol, and the solution was filtered through Celite. The filtrate was concentrated to small volume under reduced pressure. Ether was then added. The yellow solid thus formed was filtered off, washed with ether, and dried at 70 °C under high vacuum for 24 h. Yield: 0.92 g (61%). Mp: 223–225 °C dec. IR (RbI): $\nu$(Ru–Cl–Ru) 255 (br) cm$^{-1}$. Anal. Calcd for $C_{68}H_{70}Cl_4O_2P_6Ru_2$ (MW = 1449.1): C, 56.36; H, 4,87; Cl, 9.79. Found: C, 56.13; H, 4.85, Cl, 10.04. $^1$H-NMR ($CDCl_3$): $\delta$(H) = 8.23–6.56 (m, 50 H, aromatic), 3.20–1.90 (m, 16 H, $PCH_2CH_2P$), 1.83 (s, 4 H, $H_2O$). The presence of crystal water was confirmed by $^1$H-NMR. $\Lambda_M$ = 69 ($MeNO_2$).

**From *cis*-[$RuCl_2(DMSO)_4$].** *cis*-[$RuCl_2(DMSO)_4$] (3.01 g, 6.21 mmol) was suspended in dry toluene (40 mL) and heated to refluxing temperature. ETP (3.36 g, 6.29 mmol), dissolved in toluene (60 mL), was then added slowly over 1 h and the mixture was refluxed for 68 h. The yellow solid was filtered off and dissolved in 150 mL of hot ethanol. The solution was filtered through Celite to remove some insoluble material, the yellow filtrate was concentrated to ca. 10 mL under reduced pressure, and ether (200 mL) was added. The yellow product thus obtained was filtered off and dried under high vacuum at 80 °C for 12 h. (2.85 g). An additional 0.42 g of product was obtained by chromatographing the original mother liquor through silica gel. Total yield: 3.27 g (73%). The microanalytical, IR, and $^{31}$P{$^1$H}-NMR ($CDCl_3$) and $^1$H-NMR ($CDCl_3$) data are in agreement with those given above.

**[$Ru_2(\mu\text{-}Cl)_3(ETP)_2$]($CF_3SO_3$) (8).** [$Ru_2(\mu\text{-}Cl)_3(ETP)_2$]Cl·2$H_2O$ (0.1046 g, 0.0721 mmol) and $AgCF_3SO_3$ (0.0193 g, 0.075 mmol) were suspended in acetone (15 mL) and stirred at room temperature for 4.5 h, and the solution was filtered through Celite. The yellow filtrate was evaporated to dryness under reduced pressure. The resulting yellow solid was dissolved in $CH_2Cl_2$ (10 mL) and toluene (2 mL), and the solution was filtered through Celite again. The filtrate was evaporated by gentle heating and a crystalline yellow solid formed gradually. The solid was filtered off, washed with ether and dried under high vacuum at 80°C for 20 h. Yield: 0.098 g (89%). IR (RbI): $\nu$(Ru–Cl–Ru) 250 (br) cm$^{-1}$; $\nu$($CF_3SO_3$) 1263 and 1149 cm$^{-1}$. Anal. Calcd for $C_{69}H_{66}Cl_3F_3O_3P_6SRu_2$ (MW = 1526.6): C, 54.28; H, 4.36. Found: C, 53.67; H, 4.57. $^1$H-NMR ($CDCl_3$): $\delta$(H) = 8.3–7.9 and 7.7–6.8 (m, 50 H, aromatic), 3.1–1.45 (m, 16 H, $PCH_2CH_2P$). $\Lambda_M$ = 61 ($MeNO_2$).

Crystals suitable for X-ray diffraction were obtained by slow evaporation of a solution of **8** in a mixture of $CH_2Cl_2$, $CHCl_3$, and toluene.

**[$Ru_2(\mu\text{-}Cl)_3(ETP)_2$](camphorsulfonate) (9).** This complex, a yellow solid, was prepared as described for **8**. Yield: 90%. IR (RbI): $\nu$(Ru–Cl–Ru) 245 (br) cm$^{-1}$; $\nu$(CO) 1735 cm$^{-1}$; $\nu$($SO_3$) 1190 cm$^{-1}$. Anal. Calcd for $C_{78}H_{81}Cl_3O_4P_6SRu_2$ (MW = 1608.9): C, 58.23; H, 5.07; Cl 6.61. Found: C, 58.12; H, 5.35; Cl, 6.36. $^1$H-NMR ($CDCl_3$): $\delta$(H) = 8.27–8.04 (m. 3 H aromatic), 7.54–6.74 (m, 47 H, aromatic), 3.75 (s), 3.44

**Table VIII.** Final Positional and Isotropic Equivalent Displacement Parameters for the Complex [Ru(MeCN)$_3$(ETP)](CF$_3$SO$_3$)$_2$ (3)[a]

| atom | *x* | *y* | *z* | *B*, Å$^2$ | atom | *x* | *y* | *z* | *B*, Å$^2$ |
|---|---|---|---|---|---|---|---|---|---|
| Ru | 0.1762(1) | 0.25851(9) | 0.45830(9) | 3.13(3) | C(214) | −0.034(3) | 0.512(3) | 0.325(3) | 15(2)* |
| P(1) | 0.2920(4) | 0.2963(3) | 0.5404(3) | 3.6(1) | C(215) | −0.050(4) | 0.458(3) | 0.369(3) | 16(2)* |
| P(3) | 0.2646(4) | 0.2143(3) | 0.3593(3) | 4.2(1) | C(216) | 0.028(3) | 0.412(3) | 0.411(3) | 14(1)* |
| P(2) | 0.1956(4) | 0.3637(3) | 0.3953(3) | 4.2(1) | C(311) | 0.362(1) | 0.160(1) | 0.383(1) | 4.5(5)* |
| N(1) | 0.063(1) | 0.237(1) | 0.387(1) | 5.0(5) | C(312) | 0.444(2) | 0.190(1) | 0.387(1) | 5.5(6)* |
| N(3) | 0.083(1) | 0.294(1) | 0.543(1) | 5.7(5) | C(313) | 0.519(2) | 0.146(2) | 0.408(2) | 6.5(6)* |
| N(2) | 0.157(1) | 0.157(1) | 0.513(1) | 4.9(5) | C(314) | 0.506(2) | 0.072(2) | 0.422(2) | 7.0(7)* |
| C(1) | 0.349(1) | 0.370(1) | 0.491(1) | 4.7(5) | C(315) | 0.423(2) | 0.048(2) | 0.414(2) | 8.6(8)* |
| C(2) | 0.277(2) | 0.420(1) | 0.453(1) | 5.4(6) | C(316) | 0.345(2) | 0.087(2) | 0.396(2) | 6.6(6)* |
| C(3) | 0.310(2) | 0.290(1) | 0.304(1) | 5.2(6) | C(321) | 0.204(1) | 0.159(1) | 0.285(1) | 4.9(5)* |
| C(4) | 0.238(2) | 0.348(2) | 0.292(1) | 6.3(7) | C(322) | 0.219(2) | 0.169(2) | 0.204(2) | 6.5(6)* |
| C(5) | −0.000(2) | 0.228(2) | 0.352(2) | 7.6(8) | C(323) | 0.170(2) | 0.121(2) | 0.149(2) | 7.2(7)* |
| C(6) | −0.085(2) | 0.218(3) | 0.304(3) | 18(2) | C(324) | 0.117(2) | 0.071(2) | 0.171(2) | 7.6(7)* |
| C(7) | 0.137(2) | 0.111(1) | 0.547(1) | 6.1(7) | C(325) | 0.100(2) | 0.065(2) | 0.261(2) | 9.6(9)* |
| C(8) | 0.108(3) | 0.045(2) | 0.593(2) | 12(1) | C(326) | 0.150(2) | 0.103(2) | 0.317(2) | 7.2(7)* |
| C(9) | 0.029(2) | 0.294(2) | 0.588(2) | 11(1) | S(1) | 0.0712(7) | 0.1077(7) | −0.1789(7) | 10.9(3)* |
| C(10) | −0.022(2) | 0.289(3) | 0.663(2) | 14(1) | C(1) | 0.081(2) | 0.033(1) | −0.207(2) | 11.3(7)* |
| C(111) | 0.382(1) | 0.239(1) | 0.574(1) | 4.6(4)* | C(2) | 0.102(3) | 0.150(2) | −0.241(3) | 19(1)* |
| C(112) | 0.467(2) | 0.263(1) | 0.578(2) | 6.0(6)* | C(3) | −0.005(3) | 0.117(3) | −0.150(3) | 21(2)* |
| C(113) | 0.536(2) | 0.215(2) | 0.609(2) | 8.2(8)* | C(s1) | 0.109(3) | 0.106(3) | −0.102(3) | 14(1)* |
| C(114) | 0.517(2) | 0.153(2) | 0.636(2) | 7.7(7)* | F(1) | 0.209(2) | 0.085(2) | −0.085(2) | 16.2(9)* |
| C(115) | 0.436(2) | 0.126(2) | 0.634(2) | 8.5(8)* | F(2) | 0.123(2) | 0.175(2) | −0.067(2) | 17.6(9)* |
| C(116) | 0.364(2) | 0.173(2) | 0.595(2) | 6.9(7)* | F(3) | 0.066(2) | 0.057(2) | −0.054(2) | 19(1)* |
| C(121) | 0.259(1) | 0.333(1) | 0.636(1) | 3.4(4)* | S(2) | −0.211(1) | 0.122(1) | 0.553(1) | 18.9(6)* |
| C(122) | 0.280(1) | 0.402(1) | 0.661(1) | 4.6(5)* | O(4) | −0.269(3) | 0.092(2) | 0.617(3) | 20(1)* |
| C(123) | 0.257(2) | 0.426(1) | 0.734(2) | 5.9(6)* | O(5) | −0.264(2) | 0.097(2) | 0.487(2) | 13.0(8)* |
| C(124) | 0.211(1) | 0.384(1) | 0.785(1) | 5.1(5)* | O(6) | −0.230(2) | 0.203(2) | 0.576(2) | 16(1)* |
| C(125) | 0.190(2) | 0.313(1) | 0.766(2) | 5.6(6)* | C(s2) | −0.123(4) | 0.107(4) | 0.572(4) | 18(2)* |
| C(126) | 0.216(2) | 0.290(1) | 0.689(1) | 5.2(5)* | F(4) | −0.085(3) | 0.138(3) | 0.482(3) | 24(2)* |
| C(211) | 0.103(2) | 0.425(1) | 0.375(2) | 6.1(6)* | F(5) | −0.070(3) | 0.119(3) | 0.629(3) | 27(2)* |
| C(212) | 0.123(2) | 0.481(2) | 0.315(2) | 10(1)* | F(6) | −0.109(3) | 0.027(3) | 0.552(3) | 25(2)* |
| C(213) | 0.037(4) | 0.524(3) | 0.298(4) | 18(2)* | | | | | |

[a] Values marked with an asterisk denote atoms that were refined isotropically. Values for anisotropically refined atoms are given in the form of the isotropic equivalent displacement parameter defined as $(4/3)[a^2B(1,1) + b^2B(2,2) + c^2B(3,3) + ab(\cos\gamma)B(1,2) + ac(\cos\beta)B(1,3) + bc(\cos\alpha)B(2,3)]$. Atoms labeled C(s*n*) are the carbon atoms of the counterions.

(d, 1 H), 3.01–2.75 (m, 5 H), 2.75–1.50 (m, 17 H), 1.42–1.24 (m, 2 H), 1.23 (s, 3 H), 0.85 (s, 3H). $\Lambda_M$ = 46 (MeNO$_2$).

**[Ru$_2$(μ-Cl)$_3$(ETP)$_2$][BPh$_4$]·2H$_2$O (10).** This complex, a yellow solid, was prepared as described for **8**. Yield: 92%. IR (RbI): ν(Ru–Cl–Ru) 255 (br) cm$^{-1}$. Anal. Calcd for C$_{92}$H$_{90}$Cl$_3$BO$_2$P$_6$Ru$_2$ (MW = 1732.8): C, 63.77; H, 5.24. Found: C, 63.66; H, 5.10. $^1$H-NMR (CDCl$_3$): δ(H) = 8.2–6.7 (m, 70 H, aromatic), 3.3–1.1 (m, 16 H, PCH$_2$CH$_2$P), 1.54 (s, 4 H, H$_2$O). The presence of crystal water was confirmed by $^1$H-NMR. $\Lambda_M$ = 50 (MeNO$_2$).

**[RuCl$_2$(Py)(ETP)] (16).** [Ru$_2$(μ-Cl)$_3$(ETP)$_2$]Cl·2H$_2$O (0.1940 g, 0.1338 mmol), dissolved in a mixture of CH$_2$Cl$_2$ (20 mL) and pyridine (10 mL), was stirred at room temperature for 3 days. The solution was filtered through Celite. The yellow filtrate was concentrated to ca. 5 mL under reduced pressure. Ether (100 mL) and hexane (100 mL) were then added to the residue. The resulting yellow solid was filtered off and dried at room temperature over P$_2$O$_5$ for ca. 12 h. Yield: 0.2014 g, (96%). IR (RbI): ν(Ru–Cl) 274 and 244 cm$^{-1}$. Anal. Calcd for C$_{39}$H$_{38}$Cl$_2$NP$_3$Ru (MW = 785.6): C, 59.62; H, 4.88; N, 1.78; Cl, 9.03. Found: C, 58.67; H, 5.01, N, 2.10; Cl, 9.17. $^1$H-NMR (CDCl$_3$): δ(H) = 8.7–8.4 (m, 2 H), 8.24 (t, 2 H), 7.89 (t, 2 H), 7.75 (t, 2 H), 7.4–6.45 (m, 18 H), 6.65 (t, 2 H), 6.51 (t, 2 H), 3.2–2.1 (m, 6 H), 1.7–0.8 ppm (m, 2 H).

**[Ru(MeCN)$_3$(ETP)](CF$_3$SO$_3$)$_2$ (3).** [Ru$_2$(μ-Cl)$_3$(ETP)$_2$]Cl·2H$_2$O (0.4491 g, 0.3099 mmol) and silver trifluoromethanesulfonate (0.4028 g, 1.568 mmol) were dissolved in freshly distilled MeCN (20 mL). An AgCl precipitate formed immediately. The mixture was refluxed for 24 h and then filtered through Celite. The filtrate was concentrated to dryness under reduced pressure. The resulting sticky solid was dissolved in MeCN (ca. 8 mL) and filtered through a pipette containing Celite. Ether (150 mL) was slowly added to the filtrate. A white solid formed on standing overnight. This solid was filtered off, washed with ether (20 mL), and dried at room temperature over P$_2$O$_5$ for 12 h. Yield: 0.621 g (95%). IR (KBr): ν(CN) 2315 and 2287 cm$^{-1}$; ν(CF$_3$SO$_3$) 1257 and 1154 cm$^{-1}$. Anal. Calcd for C$_{42}$H$_{42}$F$_6$N$_3$O$_6$P$_3$RuS$_2$ (MW = 1056.9): C, 47.73; H, 4.01; N, 3.98; Found: C, 47.36; H, 4.29; N, 3.90. $^1$H-NMR (CDCl$_3$): δ(H) =7.66–6.92 (m,25 H, aromatic), 3.40–2.90 (m, 4 H, PCH$_2$CH$_2$P), 2.89 (s,CH$_3$CN), 2.70–2.10 (m, 4 H, PCH$_2$CH$_2$P), 2.00 (s, free CH$_3$CN), 1.83 (s,CH$_3$CN), 1.71 ppm (s, CH$_3$CN). $^1$H-NMR (CD$_3$CN): δ(H) =7.68–6.98 (m, 25 H, aromatic), 3.44–2.79 (m, 4 H, PCH$_2$CH$_2$P), 2.80 (s, CH$_3$CN), 2.55–2.24 (m, 4 H, PCH$_2$CH$_2$P), 2.22 (s, CH$_3$CN), 1.97 (free CH$_3$CN). $^{31}$P(MAS)-NMR: δ(P) = 96, 63, 59. $^{19}$F-NMR (CDCl$_3$): δ(F) = −78.32, −78.56 in a ratio of ca. 6:1. $^{19}$F-NMR (CD$_3$CN): δ(F) = −78.61. $\Lambda_M$ = 261 (MeCN).

Single crystals suitable for X-ray diffraction were obtained by slow evaporation of a solution of this complex in a solvent mixture of CH$_2$Cl$_2$, MeCN, and toluene.

**[Ru(CF$_3$SO$_3$)(MeCN)$_2$(ETP)](CF$_3$SO$_3$) (7).** It was obtained by heating crude [Ru(MeCN)$_3$(ETP)](CF$_3$SO$_3$)$_2$ (**3**), prepared as described above, under high vacuum at ca. 100 °C for 2 days. Yield: 86% based on **3**. IR (KBr): ν(CN) 2316 and 2285 cm$^{-1}$; ν(CF$_3$SO$_3$) 1278 and 1158 cm$^{-1}$. Anal. Calcd for C$_{40}$H$_{39}$F$_6$N$_2$O$_6$P$_3$RuS$_2$ (MW = 1015.9): C, 47.29; H, 3.87, N, 2.76. Found: C, 46.53; H, 3.95; N, 2.48. $^1$H-NMR (CDCl$_3$): δ(H) = 7.75–6.91(m, 25 H, aromatic), 3.50–2.80 (m, 4 H, PCH$_2$CH$_2$P), 2.70–2.10 (m, 4 H, PCH$_2$CH$_2$P), 1.72 (s, 6H, CH$_3$CN). $^{19}$F-NMR (CDCl$_3$): δ(F) = −78.24, −78.56.

***fac*-[RuCl$_2$(TTP)] (6).** A stock solution of TTP in benzene (1.35 mL × 0.16 M, 0.216 mmol) was added, at room temperature, to the yellow suspension of *cis*-[RuCl$_2$(DMSO)$_4$] (0.1010 g, 0.2084 mmol) in acetone (15 mL). The solid disappeared rapidly, and the resulting orange-red solution was refluxed for 20 min, some orange solid formed. Refluxing was continued for 30 h. The orange product was filtered off, washed with acetone and ether, and dried at ca. 80 °C overnight. Yield: 0.11 g (72%). IR (RbI): ν(Ru-Cl) 290 and 244 cm$^{-1}$. Anal. Calcd for C$_{36}$H$_{37}$Cl$_2$P$_3$Ru (MW = 734.5): C, 58.86; H, 5.08. Found: C, 58.37; H, 5.19. $\Lambda_M$ = 115 (MeCN).

Single crystals suitable for X-ray dffraction were grown by slow evaporation of a solution of this complex in a solvent mixture of CH$_2$Cl$_2$, CH$_3$CN, and toluene. This treatment did not change either composition or structure. The microanalytical, IR, and $^{31}$P-NMR (CDCl$_3$/MeCN) data for this sample were identical with those of the sample prepared as described above.

***fac*-[Ru(MeCN)$_3$(TTP)](CF$_3$SO$_3$)$_2$ (4).** [RuCl$_2$(TTP)] (0.0693 g, 0.0943 mmol) and AgCF$_3$SO$_3$ (0.0548 g, 0.2132 mmol) were suspended in MeCN (15 mL), and refluxed for 24 h. The suspension was filtered through Celite, and the filtrate was concentrated to dryness under reduced pressure. The residual sticky oil was taken up in MeCN (ca. 8 mL) and the solution was flitered again through Celite. Ether (130 mL) was slowly added to the flitrate, and the solution was left overnight. The pale solid formed was filtered off, washed with ether (10 mL), and dried at room temperature over P$_2$O$_5$ for 12 h. Yield: 0.086 g (84%). IR (KBr): ν(CN) 2316 and 2284 cm$^{-1}$; ν(CF$_3$SO$_3$) 1253 and 1159 cm$^{-1}$. Anal.

**Table IX.** Final Positional and Isotropic Equivalent Displacement Parameters for the Complex *fac*-[$RuCl_2$(TTP)] (**6**)[a]

| atom | *x* | *y* | *z* | *B*, Å$^2$ | atom | *x* | *y* | *z* | *B*, Å$^2$ |
|---|---|---|---|---|---|---|---|---|---|
| Ru | 0.363 | −0.04795(5) | 0.534 | 1.902(9) | C(124) | 0.4749(5) | 0.426(1) | 0.7590(5) | 4.4(2) |
| Cl(1) | 0.4311(1) | −0.2529(2) | 0.5578(1) | 3.24(4) | C(125) | 0.4823(4) | 0.294(1) | 0.7748(5) | 4.1(2) |
| Cl(2) | 0.3623(1) | −0.1224(2) | 0.6549(1) | 3.44(4) | C(126) | 0.4300(4) | 0.2103(9) | 0.7038(5) | 3.2(2) |
| P(1) | 0.30345(9) | 0.1389(2) | 0.5301(1) | 2.27(4) | C(211) | 0.1953(4) | −0.1976(8) | 0.3828(4) | 2.8(2) |
| P(2) | 0.2673(1) | −0.0920(2) | 0.3913(1) | 2.38(4) | C(212) | 0.2218(4) | −0.2956(9) | 0.4467(5) | 3.5(2) |
| P(3) | 0.42776(9) | 0.0307(2) | 0.4846(1) | 2.20(4) | C(213) | 0.1685(5) | −0.380(1) | 0.4426(5) | 4.3(2) |
| C(1) | 0.2468(4) | 0.2327(8) | 0.4238(5) | 3.0(2) | C(214) | 0.0905(4) | −0.364(1) | 0.3748(5) | 4.4(2) |
| C(2) | 0.2130(4) | 0.0449(9) | 0.3133(4) | 3.0(2) | C(215) | 0.0642(4) | −0.269(1) | 0.3101(6) | 4.4(2) |
| C(3) | 0.1826(4) | 0.1487(9) | 0.3438(5) | 3.3(2) | C(216) | 0.1158(4) | −0.1884(9) | 0.3134(5) | 3.5(2) |
| C(4) | 0.2947(4) | −0.1894(9) | 0.3322(4) | 3.3(2) | C(311) | 0.4153(4) | 0.1955(8) | 0.4389(4) | 2.7(2) |
| C(5) | 0.3476(4) | −0.117(1) | 0.3174(4) | 3.3(2) | C(312) | 0.4372(4) | 0.3016(9) | 0.4978(4) | 3.3(2) |
| C(6) | 0.4267(4) | −0.0753(8) | 0.4043(4) | 3.0(2) | C(313) | 0.4301(4) | 0.4307(9) | 0.4679(6) | 4.1(2) |
| C(111) | 0.2292(3) | 0.1260(8) | 0.5483(4) | 2.6(2) | C(314) | 0.4062(5) | 0.455(1) | 0.3827(6) | 4.5(2) |
| C(112) | 0.1873(4) | 0.0135(9) | 0.5297(5) | 3.4(2) | C(315) | 0.3874(5) | 0.3498(9) | 0.3253(5) | 3.9(2) |
| C(113) | 0.1266(4) | 0.011(1) | 0.5335(6) | 4.6(2) | C(316) | 0.3903(4) | 0.224(1) | 0.3519(5) | 3.6(2) |
| C(114) | 0.1078(4) | 0.123(1) | 0.5585(6) | 5.1(3) | C(321) | 0.5320(4) | 0.0418(8) | 0.5792(4) | 2.8(2) |
| C(115) | 0.1482(4) | 0.237(1) | 0.5753(5) | 4.0(2) | C(322) | 0.5829(4) | 0.102(1) | 0.5678(5) | 4.0(2) |
| C(116) | 0.2081(4) | 0.2385(9) | 0.5717(5) | 3.6(2) | C(323) | 0.6609(5) | 0.115(1) | 0.6389(6) | 4.8(2) |
| C(121) | 0.3708(3) | 0.2578(8) | 0.6185(4) | 2.7(2) | C(324) | 0.6900(5) | 0.064(1) | 0.7239(6) | 4.5(3) |
| C(122) | 0.3664(4) | 0.3919(9) | 0.6059(5) | 3.6(2) | C(325) | 0.6409(5) | 0.005(1) | 0.7357(6) | 4.2(3) |
| C(123) | 0.4175(5) | 0.4766(9) | 0.6750(5) | 4.2(2) | C(326) | 0.5619(4) | −0.0045(9) | 0.6644(5) | 3.4(2) |

[a] Esd's on the last significant digit are given in parentheses. Values for anisotropically refined atoms are given in the form of the isotropic equivalent displacement parameter defined as $(4/3)[a^2B(1,1) + b^2B(2,2) + c^2B(3,3) + ab(\cos\gamma)B(1,2) + ac(\cos\beta)B(1,3) + bc(\cos\alpha)B(2,3)]$.

Calcd for $C_{44}H_{46}F_6N_3O_6P_3RuS_2$ (MW = 1085.0): C, 48.71; H, 4.27; N, 3.87. Found: C, 48.00; H, 4.35; N, 3.85. $^1$H-NMR ($CDCl_3$): δ(H) = 7.82–7.23 (m, 25 H, aromatic), 3.10–1.40 (m, 12 H, $PCH_2CH_2CH_2P$), 2.19(s, 6 H, $CH_3CN$), 2.00 (s, 3 H, $CH_3CN$). $\Lambda_M$ = 258 (MeCN).

**Crystallography.** Crystals suitable for X-ray diffraction were obtained as described earlier and are stable in air.

All crystals were mounted on glass fibers at a random orientation, on an Enraf-Nonius CAD4 diffractometer for the unit cell and space group determinations and for data collections. Unit cell dimensions were obtained by least squares fit of the 2θ values of 25 high-order reflections ($9.43 < \theta < 16.06$ for **3**, $9.63 < \theta < 15.67$ for **6**, and $9.45 < \theta < 17.23$ for **8a**, respectively) using the CAD4 centering routines. Selected crystallographic and other relevant data are listed in Table VI and Supplementary Table S1.

Data were measured with variable scan speed to ensure constant statistical precision on the collected intensities. Three standard reflections were used to check the stabilities of the crystals and of the experimental conditions and were measured every hour. The orientation of the crystals were checked by measuring three reflections every 360 measurements. Data were corrected for Lorentz and polarization factors using the data reduction programs of the MOLEN crystallographic package.[27] Empirical absorption corrections were applied to the data sets by using azimuthal (Ψ) scans of "high-χ" angle reflections (three reflections having $\chi > 86°$, $8.8 < \theta < 15.5°$ for **3**, two reflections with $\chi > 89.3°$, $8.5 < \theta < 17.1°$ for **6**, and four reflections having $\chi > 87°$, $11.1 < \theta < 21.3°$ for **8a**).

The standard deviations on intensities were calculated in terms of statistics alone, while those on $F_o$ were calculated as shown in Table VI and Table S1.

The structures were solved by a combination of Patterson and Fourier methods and refined by full matrix least-squares[27] minimizing the function $\Sigma[w(F_o - 1/kF_c)^2]$. No extinction correction was applied. The scattering factors used, corrected for the real and imaginary parts of the anomalous dispersion, were taken from ref 28.

All calculations were carried out using the Enraf-Nonius MOLEN programs.[27]

**Structural Study of 3.** It proved impossible to obtain good quality crystals of compound **3**.

A total of 6666 independent data were collected of which 3113 were considered as observed having $|F_o^2| > 3.5\sigma|F^2|$ and used for the refinement. The structure was found to be highly disordered as can be judged from the high values of the displacement parameters of few carbon atoms of the ligands and of the two triflate counterions. It was not possible to model the different orientations of the sulphonate, and only the strongest peaks were retained and refined but led only to an approximate geometry for these moieties.

During the refinement anisotropic temperature factors were used for the Ru and P atoms as well as the ethylene groups and MeCN; isotropic factors were used for the others. The contribution of the hydrogen atoms in calculated positions (C–H = 0.95 Å, $B(H) = 1.3\,B(C_{bonded})$ (Å$^2$)) was taken into account but not refined.

Final atomic coordinates and equivalent thermal factors are given in Table VII.

**Structural Study of 6.** A total of 2865 independent reflections were collected and after data reduction 2237 were considered as observed having $|F_o^2| > 2.5\sigma|F^2|$.

The structure was refined as described above, using anisotropic factors for all atoms while the contribution of the hydrogen atoms, in idealized positions, was taken into account but not refined.

The handedness of the crystal was tested by refining the two possible sets of coordinates, those giving the lowest $R_w$ factors[29] are listed in Table VIII.

**Structural Study of 8a·$CH_2Cl_2$.** A total of 9841 independent data were collected of which 7548 were considered as observed having $|F_o^2| > 2.5\sigma|F^2|$.

During the refinement all the atoms were treated anisotropically with the hydrogen atoms contribution added as above.

Final atomic coordinates and equivalent isotropic thermal factors are given in Table IX.

**Acknowledgment.** The authors acknowledge the support of the Swiss National Science Foundation (Q.J.) and of the Italian National Research Council (A.A.). They also express their thanks to Dr. W. Amrein for the measurements of the mass spectra.

**Supplementary Material Available:** Tables giving full experimental data for compounds **3**, **6**, and **8a·$CH_2Cl_2$** (Table S1), anisotropic displacement parameters for **3** (Table S2), calculated positional parameters for the H-atoms for **3** (Table S3), extended listing of bond lengths and angles for **3** (Table S4 and S5), anisotropic displacement parameters for **6** (Table S6), calculated positional parameters for the H-atoms for **6** (Table S7), an extended listing of bond lengths, angles, and torsion angles for **6** (Tables S8–S10), anisotropic diplacement parameters for **8a·$CH_2Cl_2$** (Table S11), calculated positional parameters for the H-atoms for **8a·$CH_2Cl_2$** (Table S12), an extended listing of bond lengths, angles, and torsion angles for **8a·$CH_2Cl_2$** (Tables S13–S15) and figures giving full numbering schemes for **3** (Figure S1), **6** (Figure S2), and **8a·$CH_2Cl_2$** (Figure S3) (43 pages). Ordering information is given on any current masthead page. Tables of final observed and calculated structure factors for **3**, **6** and **8a·$CH_2Cl_2$** are available from A.A. upon request.

---

(27) MOLEN: Molecular Structure Solution Procedure: Enraf-Nonius, Delft, The Netherlands, **1990**.

(28) *International Tables for X-Ray Crystallography*; Kynoch: Birmingham, England, 1974, Vol. IV.

(29) Hamilton, W. C. *Acta Cristallogr.* **1965**, *18*, 502.